Int. J. Fuzzy Syst.
https://doi.org/10.1007/s40815-024-01840-x

Relaxed Stability and Non-weighted L_2-Gain Analysis for Asynchronously Switched Polynomial Fuzzy Systems

Zhiyong Bao[1] · **Hak-Keung Lam**[2] · **Xiaomiao Li**[1] · **Fucai Liu**[1]

Received: 10 October 2023 / Revised: 18 June 2024 / Accepted: 4 August 2024

Abstract This paper concerns the stability and non-weighted L_2-gain analysis issues for the switched systems subject to asynchronous switching and external disturbance. By taking full advantage of the admissible edge-dependent average dwell time (AED-ADT) switching signal, a stability criterion of asynchronously switched systems is proposed to achieve a lower non-weighted L_2-gain index than the existing results. Furthermore, the dynamics of switched systems are described by using the polynomial fuzzy model instead of the T-S fuzzy model, which can represent a wider range of nonlinear plants. For such asynchronously switched polynomial fuzzy systems, the relaxed conditions are derived through the membership-function-dependent (MFD) technique and novel high-order multiple Lyapunov functions (MLFs) construction method to guarantee less conservative stability and non-weighted L_2-gain results. Finally, the superiority of the proposed approaches are verified through two simulation examples.

Keywords Asynchronously switched polynomial fuzzy systems · Stability analysis · Non-weighted L_2-gain analysis · High-order multiple Lyapunov functions (MLFs)

✉ Hak-Keung Lam
hak-keung.lam@kcl.ac.uk

Zhiyong Bao
zybao@ysu.edu.cn

Xiaomiao Li
xiaomiaoli@ysu.edu.cn

Fucai Liu
lfc@ysu.edu.cn

[1] School of Electrical Engineering, Yanshan University, Qinhuangdao 066004, Hebei, China

[2] Department of Engineering, King's College London, London WC2R 2LS, UK

1 Introduction

Switched systems include both continuous dynamics and discrete switching signal, which are widely applied in practical applications, such as multi-agent systems [1], robot manipulator systems [2], and electric vehicle energy management systems [3]. Recently, many researchers have explored various stability and stabilization issues of switched systems [4].

The external disturbance is widely present in practical systems and affects the robustness of switched systems. L_2-gain can measure the impact of the disturbance on the output of the switched systems and is another fundamental topic closely related to system stability. For a considerable period, only the weighted L_2-gain of switched systems is guaranteed, such as the weighted L_2-gain based on average dwell time (ADT) switching signal in [5] and the weighted H_∞ performance based on mode-dependent average dwell time (MDADT) switching signal in [6]. However, from the practical application perspective, the weighted L_2-gain with an additional time factor is not the expected performance index. For this reason, researchers have attempted to derive the non-weighted L_2-gain index, for instance, the results under ADT switching signal [7] and persistent dwell time (PDT) switching signal [8]. It is worth noting that the above results did not take into account the phenomenon of asynchronous switching.

The asynchronous switching is often encountered in practical systems [9]. Here, asynchrony refers to the delay between the instant of subsystem switching and controller switching due to model detection, sensor response delay, or other reasons. Considering this practical-oriented issue, researchers obtained non-weighted L_2-gain by setting the increment of the Lyapunov function at switching instant to less than one, such as the widely concerned discretized Lyapunov function in [10]. However, this approach will increase

Published online: 17 September 2024

the complexity of the Lyapunov function. When setting the increment greater than one, the non-weighted L_2-gain of asynchronously switched systems under ADT switching signal is guaranteed in [11]. Moreover, the non-weighted H_∞ performance of event-triggered switched systems based on MDADT switching signal was studied in [12], which got a lower L_2-gain index by incorporating the mode-dependent switching parameters. This means that mining the switched signal information will be beneficial for reducing the L_2-gain index, thereby improving the robustness of the system. Given this, a question arises: how to employ more switching signal information to achieve a lower non-weighted L_2-gain index for the asynchronously switched systems? This motivates us to conduct more in-depth research.

Actually, switched systems also involve nonlinearity. Combined with Takagi-Sugeno (T-S) fuzzy theory, the analysis and synthesis of switched T-S fuzzy systems have been extensively studied [13–17], such as asynchronous observer-based control [13], static output-feedback control [15], and asynchronous filtering control [16]. Recently, the switched polynomial fuzzy systems and positive switched polynomial fuzzy systems were investigated in [18] and [19], respectively. Compared with T-S fuzzy model, the quantity of fuzzy rules and structural complexity of polynomial fuzzy model are significantly reduced. However, the stability analysis of switched polynomial fuzzy systems under asynchronous switching and external disturbances have yet to be studied, and existing analysis results are conservative for this class of system.

One conservative source is the stability conditions are mostly independent of the membership functions. That is, for any shape of membership functions, the stability conditions are always valid. In general fuzzy systems, there are many approaches for incorporating membership functions into the stability analysis results, such as cross-term grouping [20], copositivity verification relaxation [21], and piecewise polynomial approximation [19,22]. However, the methods in [20] and [21] require the membership functions of the controller to be parallel distributed compensated. Further, the approaches in [19] and [22] cannot guarantee the global asymptotic stability of the switched polynomial fuzzy systems. At present, there is limited research on the stability conditions of switched fuzzy systems that depend on membership functions, which is worth further exploration.

Another conservative source is the MLFs construction method. Based on the linear matrix inequality (LMI) method, the stability analysis results of asynchronously switched T-S fuzzy systems can be obtained by the quadratic MLFs [23] or the time-scheduled MLFs [24]. It is worth noting that the positive-definite matrices in these MLFs are constant, which is relatively conservative for the stability conditions of switched polynomial fuzzy systems. Meanwhile, the polynomial Lyapunov function is usually a rational fraction in general polynomial fuzzy systems [25], so it is not a radially unbounded function, and the corresponding $\mathscr{K}_\infty$ function cannot be found. To address this dilemma, the high-order MLFs are proposed for the switched polynomial fuzzy systems in [18], which can obtain the analysis results through a two-step procedure. However, the switched systems in [18] are synchronized and do not consider external disturbances. For the asynchronously switched polynomial fuzzy systems with external disturbances, the high-order MLFs constructed in [18] cannot handle the problem of the derivative of positive-definite polynomial matrices. How to propose a novel high-order MLF construction method is a challenge.

In this paper, based on the AED-ADT switching signal [26], a lower non-weighted L_2-gain index is guaranteed, which can incorporate the admissible transition edge information into the results. Next, the dynamics of asynchronously switched systems are described by the polynomial fuzzy model to represent a wider plant. Then, for such switched polynomial fuzzy systems, the analysis results are relaxed by the proposed MFD conditions and novel high-order MLFs construction method. The main contributions are outlined below.

(1) The non-weighted L_2-gain index of asynchronously switched systems is obtained by employing the AED-ADT switching signal, which can obtain a lower index than the results based on ADT and MDADT switching signals [11,12].
(2) The asynchronously switched systems are described by the polynomial fuzzy model for the first time, which helps to reduce the number of fuzzy rules and structural complexity.
(3) For the asynchronously switched polynomial fuzzy systems, a novel high-order MLFs construction method and the MFD conditions are proposed, which reduces the conservativeness of stability and L_2-gain analysis results.

The subsequent sections are arranged as follows. Section 2 gives the preliminaries. Section 3 gives the non-weighted L_2-gain index for the asynchronously switched systems and the relaxed conditions for the asynchronously switched polynomial fuzzy systems. Section 4 provides two simulation examples to validate the developed method. Section 5 draws a conclusion.

Notations: $\mathbb{Z}^+$ represents the set of positive integers. $\mathbf{I}_{n\times m}$ and $\mathbf{0}_{n\times m}$ are the identity matrix and zero matrix, respectively. A class $\mathscr{K}_\infty$ function refers to it being continuous, unbounded, strictly increasing. A sum-of-square (SOS) polynomial $\mathbf{s}(\mathbf{x})$ refers to $\mathbf{s}(\mathbf{x}) \geq 0$, and there exists arbitrary polynomial $\mathbf{s}_i(\mathbf{x})$, such that $\mathbf{s}(\mathbf{x}) = \sum_{i=1}^{k} \mathbf{s}_i(\mathbf{x})^2$. Define $\mathbb{S}$ as a set containing arbitrary SOS polynomials. $\mathcal{L}_2[0,\infty)$ denotes the space of square-integrable functions. In addition,

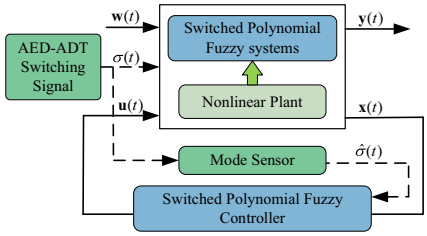

Fig. 1 The system diagram of asynchronously switched systems

an underline symbol, such as $\underline{N} = \{1, ..., N\}$, represents a finite ordered set.

2 Preliminaries

This section presents the concept of asynchronously switched systems with AED-ADT switching signals and their form described by polynomial fuzzy models. The system diagram is shown in Fig. 1.

2.1 Asynchronously Switched Systems with AED-ADT Switching Signal

Considering the switched systems as follows

$$\begin{cases} \dot{\mathbf{x}}(t) = f_{\sigma(t)}(\mathbf{x}(t), \mathbf{u}(t), \mathbf{w}(t)), \\ \mathbf{y}(t) = g_{\sigma(t)}(\mathbf{x}(t)), \end{cases} \tag{1}$$

where $\mathbf{x}(t) \in \Re^n, \mathbf{y}(t) \in \Re^\vartheta$, and $\mathbf{u}(t) \in \Re^m$ are system state, controlled output, and controlled input, respectively; $\mathbf{w}(t) \in \Re^v$ is an external disturbance which belongs to $\mathcal{L}_2[0, \infty)$. The time-dependent switching signal $\sigma(t) : [0, \infty) \to \underline{N}$ satisfies the AED-ADT property, as shown in the following definition.

Definition 1 (*see* [26]) For a switching signal $\sigma(t)$, define $N^\sigma_{q,p}(t, s)$ as the number of switches from the qth subsystem to the pth subsystem in the interval $[t, s)$, and define $T_{q,p}(t, s)$ as the total running times of the pth subsystem. Here, the pth subsystem is switched from the qth subsystem, $\forall q, p \in \underline{N} \times \underline{N}$. Thus, the switching signal $\sigma(t)$ has an AED-ADT $\tau_{q,p}$ if there exist positive numbers $N^0_{q,p}$ (the edge-dependent chatter bound) and $\tau_{q,p}$ such that

$$N^\sigma_{q,p}(t, s) \le N^0_{q,p} + \frac{T_{q,p}(t, s)}{\tau_{q,p}}. \tag{2}$$

Asynchronous switching means there is a delay between the switching time of the subsystem and the controller. Without loss of generality, assuming the switching sequence of the subsystem satisfies $t_0 < t_1 < \cdots < t_\pi < t_{\pi+1} < \cdots < +\infty$. The switching time of the controller has a delay τ_π relative to the subsystem switching. The delay $\tau_\pi = \hat{t}_\pi - t_\pi$ and satisfies $0 < \tau_\pi < t_{\pi+1} - t_\pi, \forall \pi \in \mathbb{Z}^+$. Furthermore, assuming the switched system switches from the qth subsystem to the pth subsystem at time t_π, i.e., $\sigma(t_{\pi-1}) = q$ and $\sigma(t_\pi) = p, \forall q \neq p \in \underline{N}, p \in \underline{N}$. The dynamics of asynchronously switched systems are defined as follows:

$$\begin{cases} \dot{\mathbf{x}}(t) = f_p(\mathbf{x}(t), \mathbf{u}_q(t), \mathbf{w}(t)), \\ \mathbf{y}(t) = g_p(\mathbf{x}(t)). \end{cases} \tag{3}$$

Remark 1 The control objective for the asynchronously switched system (3) is to obtain the stability criterion to guarantee the system is globally uniformly asymptotically stable (GUAS) with a lower non-weighted L_2-gain index by employing AED-ADT switching signal information.

2.2 Asynchronously Switched Polynomial Fuzzy Systems

In the following analysis, we will omit the time t associated with variables such as $\mathbf{x}(t)$, $\mathbf{u}(t)$, and $\mathbf{w}(t)$. Based on the Taylor series or sector nonlinearity approach [27], polynomial fuzzy models can describe the dynamics of switched systems (1). The fuzzy rules of the p^{th} switched polynomial fuzzy subsystem are

$$\begin{aligned} \text{Rule } R^i_p : \text{IF } & l_1(\mathbf{x}) \text{ is } L^i_{p1}, \cdots \text{and } {}_\theta(\mathbf{x}) \text{ is } L^i_{p\theta} \\ \text{THEN } & \dot{\mathbf{x}} = \mathbf{A}_{pi}(\mathbf{x})\mathbf{x} + \mathbf{B}_{pi}(\mathbf{x})\mathbf{u} + \mathbf{C}_{pi}(\mathbf{x})\mathbf{w}, \\ & \mathbf{y} = \mathbf{D}_{pi}(\mathbf{x})\mathbf{x}, \quad i \in \underline{n_p}, p \in \underline{N}, \end{aligned} \tag{4}$$

where n_p is the number of IF-THEN fuzzy rules; $L^i_{p\varsigma}, \varsigma \in \underline{\theta}$ is the fuzzy set; $\mathbf{A}_{pi}(\mathbf{x})$, $\mathbf{B}_{pi}(\mathbf{x})$, $\mathbf{C}_{pi}(\mathbf{x})$, and $\mathbf{D}_{pi}(\mathbf{x})$ are the given polynomial matrices with appropriate dimensions.

The dynamics of switched polynomial fuzzy systems is defined as

$$\dot{\mathbf{x}} = \sum_{i=1}^{n_p} \omega_{pi}(\mathbf{x})\big(\mathbf{A}_{pi}(\mathbf{x})\mathbf{x} + \mathbf{B}_{pi}(\mathbf{x})\mathbf{u} + \mathbf{C}_{pi}(\mathbf{x})\mathbf{w}\big), \tag{5}$$

$$\mathbf{y} = \sum_{i=1}^{n_p} \omega_{pi}(\mathbf{x})\mathbf{D}_{pi}(\mathbf{x})\mathbf{x}, \tag{6}$$

where $\omega_{pi}(\mathbf{x}) = \prod_{\varsigma=1}^{\theta} \mu_{L^i_{p\varsigma}}(l_\varsigma(\mathbf{x})) / \sum_{k=1}^{n_p} \prod_{\varsigma=1}^{\theta} \mu_{L^k_{p\varsigma}}(l_\varsigma(\mathbf{x}))$ is the normalized membership grade.

Next, to achieve higher design flexibility, the switched polynomial fuzzy controller is designed using the IPM concept. The fuzzy rules of the controller corresponding to the p^{th} switched polynomial fuzzy subsystem are

Rule R_p^j : IF $f_1(\mathbf{x})$ is $F_{p1}^j, \cdots$ and $f_\upsilon(\mathbf{x})$ is $F_{p\upsilon}^j$

$$\text{THEN } \mathbf{u} = \mathbf{K}_{pj}(\mathbf{x})\mathbf{x}, \quad j \in \underline{r_p},\ p \in \underline{N}, \tag{7}$$

where r_p is the number of IF-THEN fuzzy rules; $F_{p\iota}^j, \iota \in \underline{\upsilon}$ is the fuzzy set; $\mathbf{K}_{pj}(\mathbf{x})$ are the polynomial matrices to be determined. Then, the switched polynomial fuzzy controller can be obtained as

$$\mathbf{u} = \sum_{j=1}^{r_p} m_{pj}(\mathbf{x})\mathbf{K}_{pj}(\mathbf{x})\mathbf{x}, \tag{8}$$

where $m_{pj}(\mathbf{x}) = \prod_{\iota=1}^{\upsilon} \mu_{F_{p\iota}^j}(f_\iota(\mathbf{x}))/\sum_{k=1}^{r_p}\prod_{\iota=1}^{\upsilon} \mu_{F_{p\iota}^k}(f_\iota(\mathbf{x}))$ is the normalized membership grade.

From (3), (5), (6), and (8), we can get the asynchronously switched polynomial fuzzy systems as follows

$$\dot{\mathbf{x}} = \begin{cases} \sum_{i=1}^{n_p}\sum_{j=1}^{r_q} \omega_{pi}(\mathbf{x})m_{qj}(\mathbf{x})\big((\mathbf{A}_{pi}(\mathbf{x}) + \mathbf{B}_{pi}(\mathbf{x})\mathbf{K}_{qj}(\mathbf{x}))\mathbf{x} \\ \qquad +\mathbf{C}_{pi}(\mathbf{x})\mathbf{w}\big) \quad t \in [t_\pi, \hat{t}_\pi), \\ \sum_{i=1}^{n_p}\sum_{j=1}^{r_p} \omega_{pi}(\mathbf{x})m_{pj}(\mathbf{x})\big((\mathbf{A}_{pi}(\mathbf{x}) + \mathbf{B}_{pi}(\mathbf{x})\mathbf{K}_{pj}(\mathbf{x}))\mathbf{x} \\ \qquad +\mathbf{C}_{pi}(\mathbf{x})\mathbf{w}\big) \quad t \in [\hat{t}_\pi, t_{\pi+1}), \end{cases} \tag{9}$$

$$\mathbf{y} = \sum_{i=1}^{n_p} \omega_{pi}(\mathbf{x})\mathbf{D}_{pi}(\mathbf{x})\mathbf{x}. \tag{10}$$

Remark 2 The control objective for the asynchronously switched polynomial fuzzy systems (9)–(10) is to obtain the relaxed conditions and corresponding controllers based on the stability criterion in Remark 1, such that the system is GUAS with a non-weighted L_2-gain index.

3 Main Results

In this section, Theorem 1 is proposed for asynchronously switched systems to obtain a lower L_2-gain index. Theorem 2 and Theorem 3 are proposed for asynchronously switched polynomial fuzzy systems to achieve relaxed stability and L_2-gain analysis results. The graphical demonstration of the approaches and their relationship is shown in Fig. 2.

3.1 Non-weighted L_2-Gain of Asynchronously Switched Systems with AED-ADT Switching Signal

Theorem 1 *Consider the asynchronously switched systems (3), and let $\alpha_p > 0$, $\beta_p > 0$, $\mu_{[q,p]} > 1$, and $\gamma_p > 0, \forall q, p \in \underline{N}$, $q \neq p$ be given constants. If there exist continuously differentiable functions $V_{\hat{\sigma}(t)}$ and two class $\mathcal{K}_\infty$ functions k_1^p, k_2^p such that*

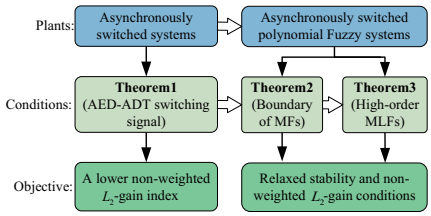

Fig. 2 The proposed approaches and their relationship diagram

$$k_1^p(\|\mathbf{x}\|) \le V_p(\mathbf{x}) \le k_2^p(\|\mathbf{x}\|), \tag{11}$$

for $\forall(\hat{\sigma}(t_\pi) = q, \hat{\sigma}(\hat{t}_\pi) = p) \in \underline{N} \times \underline{N}$, denoting $\Gamma(t) = \mathbf{y}^T\mathbf{y} - \gamma_p\mathbf{w}^T\mathbf{w}$,

$$\dot{V}_q(\mathbf{x}) \le \beta_p V_q(\mathbf{x}) - \Gamma(t) \quad t \in \mathscr{T}_\uparrow(t_\pi, t_{\pi+1}), \tag{12}$$

$$\dot{V}_p(\mathbf{x}) \le -\alpha_p V_p(\mathbf{x}) - \Gamma(t) \quad t \in \mathscr{T}_\downarrow(t_\pi, t_{\pi+1}), \tag{13}$$

and for $\forall(\hat{\sigma}(\hat{t}_\pi^-) = q, \hat{\sigma}(\hat{t}_\pi) = p) \in \underline{N} \times \underline{N}$,

$$V_p(\mathbf{x}(\hat{t}_\pi)) \le \mu_{[q,p]} V_q(\mathbf{x}(\hat{t}_\pi)), \tag{14}$$

then, for any switching signal with AED-ADT

$$\tau_{q,p} > \tau_{q,p}^* = \frac{\eta_{(q,p)}}{\alpha_p}, \tag{15}$$

the asynchronously switched system is GUAS and has a non-weighted L_2-gain index no greater than

$$\gamma = \sqrt{\frac{\alpha_{\mathrm{m}}}{-\xi_{\mathrm{m}}} e^{\sum_{p\in\underline{N}}\sum_{q\neq p, q\in\underline{N}} \eta_{(q,p)}N_{q,p}^0}}\,\gamma_{\mathrm{m}}, \tag{16}$$

where $\gamma_{\mathrm{m}} = \max_{p\in\underline{N}}\{\gamma_p\}$, $\alpha_m = \max_{p\in\underline{N}}\{\alpha_p\}$, $\xi_m = \max_{q,p\in\underline{N}, q\neq p}\{-\alpha_p + \frac{\eta_{(q,p)}}{\tau_{q,p}}\}$, $\eta_{(q,p)} = (\alpha_p + \beta_p)\mathscr{T}_m + \ln\mu_{[q,p]}$ and $\mathscr{T}_m = \max_{\forall\pi\in\mathbb{Z}^+}\{\mathscr{T}_\uparrow(t_\pi, t_{\pi+1})\}$.

Proof At first, assuming that the switching signal of the controller is denoted as $\hat{\sigma}(t) = \sigma(t - \tau_\pi), \forall\pi \in \mathbb{Z}^+$. The switched subsystem switches from the qth subsystem to the pth subsystem at time t_π. The controller switches at time $\hat{t}_\pi$, which satisfies $t_\pi < \hat{t}_\pi < t_{\pi+1}$. Then, it can be obtained that $\hat{\sigma}(\hat{t}_{\pi-1}) = \hat{\sigma}(t_\pi) = \hat{\sigma}(\hat{t}_\pi^-) = q$ and $\hat{\sigma}(\hat{t}_\pi) = p$.

For concise notation, let $\mathscr{T}_\uparrow(t_\pi, t_{\pi+1})$ denote the unmatched interval $[t_\pi, \hat{t}_\pi)$, and $\mathscr{T}_\downarrow(t_\pi, t_{\pi+1})$ represent the matched interval $[\hat{t}_\pi, t_{\pi+1})$. $\mathscr{T}_\uparrow(t-\varsigma)$ represents the total length of the intervals where the Lyapunov function increases in the interval $[\varsigma, t)$, and $\mathscr{T}_\downarrow(t-\varsigma)$ represents the length of the intervals where the Lyapunov function decreases. Inspired by [28], the MLFs are dependent on the switching signal of the controller $\hat{\sigma}(t)$, i.e., $V_{\hat{\sigma}(t)} : \Re^n \to \Re$, as shown in Fig. 3.

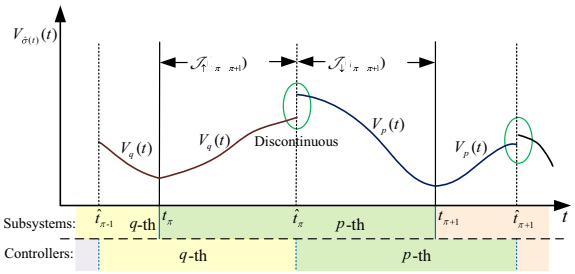

Fig. 3 The MLFs that depend on the switching signal of the controller

When $t \in [\hat{t}_\pi, t_{\pi+1}), \forall \pi \in \mathbb{Z}^+$, by integrating (13), we have

$$
\begin{aligned}
V_{\hat{\sigma}(t)}(\mathbf{x}) &\le e^{-\alpha_{\hat{\sigma}(\hat{t}_\pi)}(t-\hat{t}_\pi)} V_{\hat{\sigma}(\hat{t}_\pi)}(\mathbf{x}(\hat{t}_\pi)) - \int_{\hat{t}_\pi}^{t} e^{-\alpha_{\hat{\sigma}(\hat{t}_\pi)}(t-\varsigma)}\Gamma(\varsigma)d\varsigma \\
&\le \mu_{[\hat{\sigma}(\hat{t}_\pi^-),\hat{\sigma}(\hat{t}_\pi)]} e^{-\alpha_{\hat{\sigma}(\hat{t}_\pi)}(t-\hat{t}_\pi)} V_{\hat{\sigma}(\hat{t}_\pi^-)}(\mathbf{x}(\hat{t}_\pi)) \\
&\quad - \int_{\hat{t}_\pi}^{t} e^{-\alpha_{\hat{\sigma}(\hat{t}_\pi)}(t-\varsigma)}\Gamma(\varsigma)d\varsigma \\
&\le \mu_{[\hat{\sigma}(\hat{t}_\pi^-),\hat{\sigma}(\hat{t}_\pi)]} e^{-\alpha_{\hat{\sigma}(\hat{t}_\pi)}(t-\hat{t}_\pi)} \Big(e^{\beta_{\hat{\sigma}(\hat{t}_\pi)}(\hat{t}_\pi - t_\pi)} V_{\hat{\sigma}(t_\pi)}(\mathbf{x}(t_\pi)) \\
&\quad - \int_{t_\pi}^{\hat{t}_\pi} e^{\beta_{\hat{\sigma}(\hat{t}_\pi)}(\hat{t}_\pi-\varsigma)}\Gamma(\varsigma)d\varsigma \Big) - \int_{\hat{t}_\pi}^{t} e^{-\alpha_{\hat{\sigma}(\hat{t}_\pi)}(t-\varsigma)}\Gamma(\varsigma)d\varsigma \\
&= \mu_{[\hat{\sigma}(\hat{t}_\pi^-),\hat{\sigma}(\hat{t}_\pi)]} e^{-\alpha_{\hat{\sigma}(\hat{t}_\pi)}\mathscr{T}_{\downarrow}(t-t_\pi)+\beta_{\hat{\sigma}(\hat{t}_\pi)}\mathscr{T}_{\uparrow}(t-t_\pi)} V_{\hat{\sigma}(t_\pi)}(\mathbf{x}(t_\pi)) \\
&\quad - \mu_{[\hat{\sigma}(\hat{t}_\pi^-),\hat{\sigma}(\hat{t}_\pi)]} \int_{t_\pi}^{\hat{t}_\pi} e^{-\alpha_{\hat{\sigma}(\hat{t}_\pi)}(t-\hat{t}_\pi)+\beta_{\hat{\sigma}(\hat{t}_\pi)}(\hat{t}_\pi-\varsigma)}\Gamma(\varsigma)d\varsigma \\
&\quad - \int_{\hat{t}_\pi}^{t} e^{-\alpha_{\hat{\sigma}(\hat{t}_\pi)}(t-\varsigma)}\Gamma(\varsigma)d\varsigma \\
&\le \mu_{[\hat{\sigma}(\hat{t}_\pi^-),\hat{\sigma}(\hat{t}_\pi)]} e^{-\alpha_{\hat{\sigma}(\hat{t}_\pi)}\mathscr{T}_{\downarrow}(t-t_\pi)+\beta_{\hat{\sigma}(\hat{t}_\pi)}\mathscr{T}_{\uparrow}(t-t_\pi)} V_{\hat{\sigma}(t_\pi)}(\mathbf{x}(t_\pi)) \\
&\quad - \int_{t_\pi}^{\hat{t}_\pi} e^{-\alpha_{\hat{\sigma}(\hat{t}_\pi)}(t-\hat{t}_\pi)+\beta_{\hat{\sigma}(\hat{t}_\pi)}(\hat{t}_\pi-\varsigma)}\Gamma(\varsigma)d\varsigma \\
&\quad - \int_{\hat{t}_\pi}^{t} e^{-\alpha_{\hat{\sigma}(\hat{t}_\pi)}(t-\varsigma)}\Gamma(\varsigma)d\varsigma \\
&= \mu_{[\hat{\sigma}(\hat{t}_\pi^-),\hat{\sigma}(\hat{t}_\pi)]} e^{-\alpha_{\hat{\sigma}(\hat{t}_\pi)}\mathscr{T}_{\downarrow}(t-t_\pi)+\beta_{\hat{\sigma}(\hat{t}_\pi)}\mathscr{T}_{\uparrow}(t-t_\pi)} V_{\hat{\sigma}(t_\pi)}(\mathbf{x}(t_\pi)) \\
&\quad - \int_{t_\pi}^{t} e^{-\alpha_{\hat{\sigma}(\hat{t}_\pi)}\mathscr{T}_{\downarrow}(t-\varsigma)+\beta_{\hat{\sigma}(\hat{t}_\pi)}\mathscr{T}_{\uparrow}(t-\varsigma)}\Gamma(\varsigma)d\varsigma. \qquad (17)
\end{aligned}
$$

When $t \in [t_\pi, \hat{t}_\pi), \forall \pi \in \mathbb{Z}^+$, by integrating (12), one can obtain

$$
\begin{aligned}
V_{\hat{\sigma}(t)}(\mathbf{x}) &\le e^{\beta_{\hat{\sigma}(\hat{t}_\pi)}(t-t_\pi)} V_{\hat{\sigma}(t_\pi)}(\mathbf{x}(t_\pi)) - \int_{t_\pi}^{t} e^{\beta_{\hat{\sigma}(\hat{t}_\pi)}(t-\varsigma)}\Gamma(\varsigma)d\varsigma \\
&= e^{-\alpha_{\hat{\sigma}(\hat{t}_\pi)}\mathscr{T}_{\downarrow}(t-t_\pi)+\beta_{\hat{\sigma}(\hat{t}_\pi)}\mathscr{T}_{\uparrow}(t-t_\pi)} V_{\hat{\sigma}(t_\pi)}(\mathbf{x}(t_\pi)) \\
&\quad - \int_{t_\pi}^{t} e^{-\alpha_{\hat{\sigma}(\hat{t}_\pi)}\mathscr{T}_{\downarrow}(t-\varsigma)+\beta_{\hat{\sigma}(\hat{t}_\pi)}\mathscr{T}_{\uparrow}(t-\varsigma)}\Gamma(\varsigma)d\varsigma \\
&\le \mu_{[\hat{\sigma}(\hat{t}_\pi^-),\hat{\sigma}(\hat{t}_\pi)]} e^{-\alpha_{\hat{\sigma}(\hat{t}_\pi)}\mathscr{T}_{\downarrow}(t-t_\pi)+\beta_{\hat{\sigma}(\hat{t}_\pi)}\mathscr{T}_{\uparrow}(t-t_\pi)} V_{\hat{\sigma}(t_\pi)}(\mathbf{x}(t_\pi)) \\
&\quad - \int_{t_\pi}^{t} e^{-\alpha_{\hat{\sigma}(\hat{t}_\pi)}\mathscr{T}_{\downarrow}(t-\varsigma)+\beta_{\hat{\sigma}(\hat{t}_\pi)}\mathscr{T}_{\uparrow}(t-\varsigma)}\Gamma(\varsigma)d\varsigma. \qquad (18)
\end{aligned}
$$

Combining (17) and (18), for $t \in [t_\pi, t_{\pi+1}), \forall \pi \in \mathbb{Z}^+$, one can obtain

$$
\begin{aligned}
V_{\hat{\sigma}(t)}(\mathbf{x}) &\le \mu_{[\hat{\sigma}(\hat{t}_\pi^-),\hat{\sigma}(\hat{t}_\pi)]} e^{-\alpha_{\hat{\sigma}(\hat{t}_\pi)}\mathscr{T}_{\downarrow}(t-t_\pi)+\beta_{\hat{\sigma}(\hat{t}_\pi)}\mathscr{T}_{\uparrow}(t-t_\pi)} V_{\hat{\sigma}(\hat{t}_\pi^-)}(\mathbf{x}(t_\pi^-)) \\
&\quad - \int_{t_\pi}^{t} e^{-\alpha_{\hat{\sigma}(\hat{t}_\pi)}\mathscr{T}_{\downarrow}(t-\varsigma)+\beta_{\hat{\sigma}(\hat{t}_\pi)}\mathscr{T}_{\uparrow}(t-\varsigma)}\Gamma(\varsigma)d\varsigma \\
&\le \mu_{[\hat{\sigma}(\hat{t}_\pi^-),\hat{\sigma}(\hat{t}_\pi)]} e^{-\alpha_{\hat{\sigma}(\hat{t}_\pi)}\mathscr{T}_{\downarrow}(t-t_\pi)+\beta_{\hat{\sigma}(\hat{t}_\pi)}\mathscr{T}_{\uparrow}(t-t_\pi)} \big(\mu_{[\hat{\sigma}(\hat{t}_{\pi-1}^-),\hat{\sigma}(\hat{t}_{\pi-1})]} \\
&\quad \times e^{-\alpha_{\hat{\sigma}(\hat{t}_{\pi-1})}\mathscr{T}_{\downarrow}(t_\pi-t_{\pi-1})+\beta_{\hat{\sigma}(\hat{t}_{\pi-1})}\mathscr{T}_{\uparrow}(t_\pi-t_{\pi-1})} V_{\hat{\sigma}(\hat{t}_{\pi-1})}(\mathbf{x}(t_{\pi-1})) \\
&\quad - \int_{t_{\pi-1}}^{t_\pi} e^{-\alpha_{\hat{\sigma}(\hat{t}_{\pi-1})}\mathscr{T}_{\downarrow}(t_\pi-\varsigma)+\beta_{\hat{\sigma}(\hat{t}_{\pi-1})}\mathscr{T}_{\uparrow}(t_\pi-\varsigma)}\Gamma(\varsigma)d\varsigma\big) \\
&\quad - \int_{t_\pi}^{t} e^{-\alpha_{\hat{\sigma}(\hat{t}_\pi)}\mathscr{T}_{\downarrow}(t-\varsigma)+\beta_{\hat{\sigma}(\hat{t}_\pi)}\mathscr{T}_{\uparrow}(t-\varsigma)}\Gamma(\varsigma)d\varsigma \\
&\le \mu_{[\hat{\sigma}(\hat{t}_{\pi-1}),\hat{\sigma}(\hat{t}_\pi)]} \cdots \mu_{[\hat{\sigma}(\hat{t}_0),\hat{\sigma}(\hat{t}1)]} e^{-\alpha_{\hat{\sigma}(\hat{t}_\pi)}\mathscr{T}_{\downarrow}(t-t_\pi)+\beta_{\hat{\sigma}(\hat{t}_\pi)}\mathscr{T}_{\uparrow}(t-t_\pi)} \cdots \\
&\quad \times e^{-\alpha_{\hat{\sigma}(\hat{t}_0)}\mathscr{T}_{\downarrow}(t_1-t_0)+\beta_{\hat{\sigma}(\hat{t}_0)}\mathscr{T}_{\uparrow}(t_1-t_0)} V_{\hat{\sigma}(t_0)}(\mathbf{x}(t_0)) \\
&\quad - \mu_{[\hat{\sigma}(\hat{t}_{\pi-1}),\hat{\sigma}(\hat{t}_\pi)]} \cdots \mu_{[\hat{\sigma}(\hat{t}_1),\hat{\sigma}(\hat{t}_2)]} e^{-\alpha_{\hat{\sigma}(\hat{t}_\pi)}\mathscr{T}_{\downarrow}(t-t_\pi)+\beta_{\hat{\sigma}(\hat{t}_\pi)}\mathscr{T}_{\uparrow}(t-t_\pi)} \cdots \\
&\quad \times e^{-\alpha_{\hat{\sigma}(\hat{t}_1)}\mathscr{T}_{\downarrow}(t_2-t_1)+\beta_{\hat{\sigma}(\hat{t}_1)}\mathscr{T}_{\uparrow}(t_2-t_1)} \\
&\quad \times \int_{t_0}^{t_1} e^{-\alpha_{\hat{\sigma}(t_0)}\mathscr{T}_{\downarrow}(t_1-\varsigma)+\beta_{\hat{\sigma}(t_0)}\mathscr{T}_{\uparrow}(t_1-\varsigma)}\Gamma(\varsigma)d\varsigma \\
&\quad - \cdots - \mu_{[\hat{\sigma}(\hat{t}_{\pi-1}),\hat{\sigma}(\hat{t}_\pi)]} e^{-\alpha_{\hat{\sigma}(\hat{t}_\pi)}\mathscr{T}_{\downarrow}(t-t_\pi)+\beta_{\hat{\sigma}(\hat{t}_\pi)}\mathscr{T}_{\uparrow}(t-t_\pi)} \\
&\quad \times \int_{t_{\pi-1}}^{t_\pi} e^{-\alpha_{\hat{\sigma}(\hat{t}_{\pi-1})}\mathscr{T}_{\downarrow}(t_\pi-\varsigma)+\beta_{\hat{\sigma}(\hat{t}_{\pi-1})}\mathscr{T}_{\uparrow}(t_\pi-\varsigma)}\Gamma(\varsigma)d\varsigma \\
&\quad - \int_{t_\pi}^{t} e^{-\alpha_{\hat{\sigma}(\hat{t}_\pi)}\mathscr{T}_{\downarrow}(t-\varsigma)+\beta_{\hat{\sigma}(\hat{t}_\pi)}\mathscr{T}_{\uparrow}(t-\varsigma)}\Gamma(\varsigma)d\varsigma \\
&= e^{-\alpha_{\hat{\sigma}(\hat{t}_\pi)}\mathscr{T}_{\downarrow}(t_\pi,t)+\beta_{\hat{\sigma}(\hat{t}_\pi)}\mathscr{T}_{\uparrow}(t_\pi,t)} \\
&\quad \times \prod_{\iota=0}^{\pi-1} \mu_{[\hat{\sigma}(\hat{t}_\iota),\hat{\sigma}(\hat{t}_{\iota+1})]} e^{-\alpha_{\hat{\sigma}(\hat{t}_\iota)}\mathscr{T}_{\downarrow}(t_\iota,t_{\iota+1})+\beta_{\hat{\sigma}(\hat{t}_\iota)}\mathscr{T}_{\uparrow}(t_\iota,t_{\iota+1})} V_{\hat{\sigma}(t_0)}(\mathbf{x}(t_0)) \\
&\quad - \int_{t_0}^{t} \prod_{q\neq p,q=0}^{\pi-1} \prod_{p=0}^{\pi-1} \Big(\mu_{[\hat{\sigma}(\hat{t}_p),\hat{\sigma}(\hat{t}_{p+1})]}\Big)^{N^{\sigma}_{q,p}(\varsigma,t)} \\
&\quad \times e^{-\alpha_{\hat{\sigma}(\hat{t}_p)}(T_{\downarrow q,p}(\varsigma,t))+\beta_{\hat{\sigma}(\hat{t}_p)}T_{\uparrow q,p}(\varsigma,t)}\Gamma(\varsigma)d\varsigma \\
&= e^{\sum_{p\in\underline{N}}\sum_{q\neq p,q\in\underline{N}} N^{\sigma}_{q,p}(0,t)\ln\mu_{[q,p]}-\alpha_p T_{\downarrow q,p}(0,t)+\beta_p T_{\uparrow q,p}(0,t)} V_{\hat{\sigma}(t_0)}(\mathbf{x}(t_0)) \\
&\quad - \int_{t_0}^{t} e^{\sum_{p\in\underline{N}}\sum_{q\neq p,q\in\underline{N}} N^{\sigma}_{q,p}(\varsigma,t)\ln\mu_{[q,p]}-\alpha_p(T_{\downarrow q,p}(\varsigma,t))+\beta_p T_{\uparrow q,p}(\varsigma,t)}\Gamma(\varsigma)d\varsigma, \qquad (19)
\end{aligned}
$$

where $T_{\uparrow q,p}(\varsigma,t)$ and $T_{\downarrow q,p}(\varsigma,t)$ are the total unmatched and matched interval of pth subsystem during the interval $[\varsigma, t)$. Here, the pth subsystem is switched from the qth subsystem, $\forall q, p \in \underline{N} \times \underline{N}$.

Denoting $\mathscr{T}_{\mathrm{m}} = \max_{\forall\pi\in\mathbb{Z}^+}\{\mathscr{T}_{\uparrow}(t_\pi, t_{\pi+1})\}$ and $\eta_{(q,p)} = (\alpha_p + \beta_p)\mathscr{T}_{\mathrm{m}} + \ln\mu_{[q,p]}$. When $\mathbf{w} \equiv 0$, applying (2) to (19), we have

$$
\begin{aligned}
V_{\hat{\sigma}(t)}(\mathbf{x}) &\le e^{\sum_{p\in\underline{N}}\sum_{q\neq p,q\in\underline{N}} N^{\sigma}_{q,p}(0,t)\ln\mu_{[q,p]}+(\alpha_p+\beta_p)\mathscr{T}_{\mathrm{m}}N^{\sigma}_{q,p}(0,t)-\alpha_p(t-t_0)} \\
&\quad \times V_{\hat{\sigma}(t_0)}(\mathbf{x}(t_0)) \\
&\le e^{\sum_{p\in\underline{N}}\sum_{q\neq p,q\in\underline{N}} \eta_{(q,p)}N^0_{q,p}+(-\alpha_p+\frac{\eta_{(q,p)}}{\tau_{q,p}})(t-t_0)} V_{\hat{\sigma}(t_0)}(\mathbf{x}(t_0)). \qquad (20)
\end{aligned}
$$

If the AED-ADT switching signal satisfies (15), i.e., $-\alpha_p + \frac{\eta_{(q,p)}}{\tau_{q,p}} < 0$, $V_{\hat{\sigma}(t)}(\mathbf{x})$ approach to 0 as $t \to +\infty$. Therefore, we can obtain the asynchronously switched system is GUAS with the aid of (11).

When $\mathbf{w} \neq 0$, from (19), we obtain

$$\begin{aligned}
&\int_{t_0}^{t} e^{\sum_{p\in\underline{N}}\sum_{q\neq p,q\in\underline{N}} N^{\sigma}_{q,p}(\varsigma,t)\ln\mu_{[q,p]}-\alpha_p(T_{\downarrow q,p}(\varsigma,t))+\beta_p T_{\uparrow q,p}(\varsigma,t)} \\
&\mathbf{y}(\varsigma)^T\mathbf{y}(\varsigma)d\varsigma \\
&\leq \gamma_p^2\int_{t_0}^{t} e^{\sum_{p\in\underline{N}}\sum_{q\neq p,q\in\underline{N}} N^{\sigma}_{q,p}(\varsigma,t)\ln\mu_{[q,p]}-\alpha_p(T_{\downarrow q,p}(\varsigma,t))+\beta_p T_{\uparrow q,p}(\varsigma,t)} \\
&\mathbf{w}(\varsigma)^T\mathbf{w}(\varsigma)d\varsigma. \qquad (21)
\end{aligned}$$

For the left side of (21), we obtain

$$\begin{aligned}
&\int_{t_0}^{t} e^{\sum_{p\in\underline{N}}\sum_{q\neq p,q\in\underline{N}} N^{\sigma}_{q,p}(\varsigma,t)\ln\mu_{[q,p]}-\alpha_p(T_{\downarrow q,p}(\varsigma,t))+\beta_p T_{\uparrow q,p}(\varsigma,t)} \\
&\mathbf{y}(\varsigma)^T\mathbf{y}(\varsigma)d\varsigma \\
&\geq \int_{t_0}^{t} e^{-\alpha_{\mathrm{m}}(t-\varsigma)}\mathbf{y}(\varsigma)^T\mathbf{y}(\varsigma)d\varsigma, \qquad (22)
\end{aligned}$$

where $\alpha_{\mathrm{m}} = \max_{p\in\underline{N}}\{\alpha_p\}$.

For the right side of (21), we obtain

$$\begin{aligned}
&\gamma_p^2\int_{t_0}^{t} e^{\sum_{p\in\underline{N}}\sum_{q\neq p,q\in\underline{N}} N^{\sigma}_{q,p}(\varsigma,t)\ln\mu_{[q,p]}-\alpha_p(T_{\downarrow q,p}(\varsigma,t))+\beta_p T_{\uparrow q,p}(\varsigma,t)} \\
&\mathbf{w}(\varsigma)^T\mathbf{w}(\varsigma)d\varsigma \\
&\leq \gamma_p^2\int_{t_0}^{t} e^{\sum_{p\in\underline{N}}\sum_{q\neq p,q\in\underline{N}} N^{\sigma}_{q,p}(\varsigma,t)\ln\mu_{[q,p]}+(\alpha_p+\beta_p)\mathscr{T}_{\mathrm{m}}N^{\sigma}_{q,p}(\varsigma,t)-\alpha_p T_{q,p}(\varsigma,t)} \\
&\mathbf{w}(\varsigma)^T\mathbf{w}(\varsigma)d\varsigma \\
&= e^{\sum_{p\in\underline{N}}\sum_{q\neq p,q\in\underline{N}}\eta_{(q,p)}N^0_{q,p}}\gamma_p^2\int_{t_0}^{t} e^{\sum_{p\in\underline{N}}\sum_{q\neq p,q\in\underline{N}}(-\alpha_p+\frac{\eta_{(q,p)}}{\tau_{q,p}})T_{q,p}(\varsigma,t)} \\
&\mathbf{w}(\varsigma)^T\mathbf{w}(\varsigma)d\varsigma \\
&\leq e^{\sum_{p\in\underline{N}}\sum_{q\neq p,q\in\underline{N}}\eta_{(q,p)}N^0_{q,p}}\gamma_p^2\int_{t_0}^{t} e^{\xi_{\mathrm{m}}(t-\varsigma)}\mathbf{w}(\varsigma)^T\mathbf{w}(\varsigma)d\varsigma, \qquad (23)
\end{aligned}$$

where $\xi_{\mathrm{m}} = \max_{q,p\in\underline{N},q\neq p}\{-\alpha_p + \frac{\eta_{(q,p)}}{\tau_{q,p}}\}$.

Adding (22) and (23) to (21), we obtain

$$\begin{aligned}
&\int_{t_0}^{t} e^{-\alpha_{\mathrm{m}}(t-\varsigma)}\mathbf{y}(\varsigma)^T\mathbf{y}(\varsigma)d\varsigma \leq e^{\sum_{p\in\underline{N}}\sum_{q\neq p,q\in\underline{N}}\eta_{(q,p)}N^0_{q,p}}\gamma_p^2 \\
&\int_{t_0}^{t} e^{\xi_{\mathrm{m}}(t-\varsigma)}\mathbf{w}(\varsigma)^T\mathbf{w}(\varsigma)d\varsigma. \qquad (24)
\end{aligned}$$

Integrating (24) for t from t_0 to $+\infty$, one can obtain

$$\begin{aligned}
&\int_{t_0}^{+\infty}\int_{t_0}^{t} e^{-\alpha_{\mathrm{m}}(t-\varsigma)}\mathbf{y}(\varsigma)^T\mathbf{y}(\varsigma)d\varsigma dt \\
&\leq e^{\sum_{p\in\underline{N}}\sum_{q\neq p,q\in\underline{N}}\eta_{(q,p)}N^0_{q,p}}\gamma_p^2\int_{t_0}^{+\infty}\int_{t_0}^{t} e^{\xi_{\mathrm{m}}(t-\varsigma)}\mathbf{w}(\varsigma)^T\mathbf{w}(\varsigma)d\varsigma dt. \qquad (25)
\end{aligned}$$

This is equivalent to

$$\begin{aligned}
&\int_{t_0}^{+\infty}\int_{\varsigma}^{+\infty} e^{-\alpha_{\mathrm{m}}(t-\varsigma)}\mathbf{y}(\varsigma)^T\mathbf{y}(\varsigma)dtd\varsigma \\
&\leq e^{\sum_{p\in\underline{N}}\sum_{q\neq p,q\in\underline{N}}\eta_{(q,p)}N^0_{q,p}}\gamma_p^2\int_{t_0}^{+\infty}\int_{\varsigma}^{+\infty} e^{\xi_{\mathrm{m}}(t-\varsigma)}\mathbf{w}(\varsigma)^T\mathbf{w}(\varsigma)dtd\varsigma. \qquad (26)
\end{aligned}$$

Thus, one can obtain

$$\begin{aligned}
&\frac{1}{\alpha_{\mathrm{m}}}\int_{t_0}^{+\infty}\mathbf{y}(\varsigma)^T\mathbf{y}(\varsigma)d\varsigma \leq \frac{1}{-\xi_{\mathrm{m}}}e^{\sum_{p\in\underline{N}}\sum_{q\neq p,q\in\underline{N}}\eta_{(q,p)}N^0_{q,p}}\gamma_p^2 \\
&\int_{t_0}^{+\infty}\mathbf{w}(\varsigma)^T\mathbf{w}(\varsigma)d\varsigma. \qquad (27)
\end{aligned}$$

That is

$$\int_{t_0}^{+\infty}\mathbf{y}(\varsigma)^T\mathbf{y}(\varsigma)d\varsigma \leq \gamma^2\int_{t_0}^{+\infty}\mathbf{w}(\varsigma)^T\mathbf{w}(\varsigma)d\varsigma, \qquad (28)$$

where $\gamma = \sqrt{\frac{\alpha_{\mathrm{m}}}{-\xi_{\mathrm{m}}}e^{\sum_{p\in\underline{N}}\sum_{q\neq p,q\in\underline{N}}\eta_{(q,p)}N^0_{q,p}}}\gamma_{\mathrm{m}}$, $\gamma_{\mathrm{m}} = \max\{\gamma_p\}$.

This completes the proof. □

Remark 3 The comparison between the non-weighted L_2-gain index obtained in this paper and existing results is shown in Table 1.

When $\eta_{(q,p)} = \eta_p$, $\tau_{q,p} = \tau_p$, $\sum_{p\in\underline{N}} N^0_{q,p} = N_{0p}$, the non-weighted L_2-gain based on AED-ADT switching signal equals the one based on MDADT switching signal. Similarly, the non-weighted L_2-gain based on ADT switching signals can be seen as a special case of the non-weighted L_2-gain based on MDADT switching signals. Thus, the derived non-weighted L_2-gain in this paper is more general than the results in [11] and [12]. That is, more switching signal information can be employed to achieve a lower L_2-gain index for asynchronously switched systems. Physically speaking, a lower non-weighted L_2-gain index has more general anti-disturbance capacity and enhanced robustness to variations in external disturbance.

3.2 MFD Conditions of Asynchronously Switched Polynomial Fuzzy Systems

Theorem 2 *Consider the asynchronously switched polynomial fuzzy systems (9)–(10), and let $\mu_{[q,p]} > 1$, $\beta_p > 0$, $\alpha_p > 0$ and $\gamma_p > 0$, $\forall q \neq p$, $q, p \in \underline{N}$ be given constants. Defining the symmetric constant matrices $\mathbf{Q}_p \in \Re^{n\times n}$, arbitrary polynomial matrices $\mathbf{X}_{pj}(\mathbf{x}) \in \Re^{m\times n}$, slack polynomial matrices $\overline{\mathbf{R}}_{1pqij}(\mathbf{x})$, $\underline{\mathbf{R}}_{1pqij}(\mathbf{x})$, $q \neq p, q, p \in \underline{N}, i \in$*

Table 1 Comparison of non-weighted L_2-gain index based on different switching signals

Theorem	Switching signal	Non-weighted L_2-gain index
Theorem 2 in [11]	ADT	$\sqrt{\frac{\alpha}{-(-\alpha+\eta/\tau)}e^{\eta N_0}}\gamma_{\mathrm{m}}$
Theorem 2 in [12]	MDADT	$\sqrt{\frac{\alpha_{\mathrm{m}}}{-\xi_{\mathrm{m}}}e^{\sum_{p\in}\eta_p N_{0p}}}\gamma_{\mathrm{m}}$
Theorem 1	AED-ADT	$\sqrt{\frac{\alpha_{\mathrm{m}}}{-\xi_{\mathrm{m}}}e^{\sum_{p\in\underline{N}}\sum_{q\neq p,q\in\underline{N}}\eta_{(q,p)}N^0_{q,p}}}\gamma_{\mathrm{m}}$

$\underline{n_p}, j \in \underline{r_q}$ *and* $\overline{\mathbf{R}}_{2pij}(\mathbf{x})$, $\underline{\mathbf{R}}_{2pij}(\mathbf{x})$, $p \in \underline{N}, i \in \underline{n_p}, j \in \underline{r_p}$, *if there exist feasible solutions to the following conditions:*

$$\ell^T(\mathbf{Q}_p - \varphi_1\mathbf{I})\ell \in \mathbb{S} \quad \forall p, \tag{29}$$

$$\ell^T(\overline{\mathbf{R}}_{1pqij}(\mathbf{x}) - \varphi_2(\mathbf{x})\mathbf{I})\ell \in \mathbb{S} \quad \forall q \neq p, i, j, \tag{30}$$

$$\ell^T(\underline{\mathbf{R}}_{1pqij}(\mathbf{x}) - \varphi_3(\mathbf{x})\mathbf{I})\ell \in \mathbb{S} \quad \forall q \neq p, i, j, \tag{31}$$

$$\ell^T(\overline{\mathbf{R}}_{2pij}(\mathbf{x}) - \varphi_4(\mathbf{x})\mathbf{I})\ell \in \mathbb{S} \quad \forall p, i, j, \tag{32}$$

$$\ell^T(\underline{\mathbf{R}}_{2pij}(\mathbf{x}) - \varphi_5(\mathbf{x})\mathbf{I})\ell \in \mathbb{S} \quad \forall p, i, j, \tag{33}$$

$$\begin{aligned} &-\ell^T\big(\tilde{\Xi}_{1pqij}(\mathbf{x}) + \underline{\mathbf{R}}_{1pqij}(\mathbf{x}) - \overline{\mathbf{R}}_{1pqij}(\mathbf{x}) \\ &\quad + \sum_{r=1}^{n_p}\sum_{s=1}^{r_q}(\overline{\gamma}_{pqrs}\overline{\mathbf{R}}_{1pqrs}(\mathbf{x}) \\ &\quad - \underline{\gamma}_{pqrs}\underline{\mathbf{R}}_{1pqrs}(\mathbf{x})) + \varphi_6(\mathbf{x})\mathbf{I}\big)\ell \in \mathbb{S} \quad \forall q \neq p, i, j, \end{aligned} \tag{34}$$

$$\begin{aligned} &-\ell^T\big(\tilde{\Xi}_{2pij}(\mathbf{x}) + \underline{\mathbf{R}}_{2pij}(\mathbf{x}) - \overline{\mathbf{R}}_{2pij}(\mathbf{x}) \\ &\quad + \sum_{r=1}^{n_p}\sum_{s=1}^{r_p}(\overline{\gamma}_{prs}\overline{\mathbf{R}}_{2prs}(\mathbf{x}) - \underline{\gamma}_{prs}\underline{\mathbf{R}}_{2prs}(\mathbf{x})) + \varphi_7(\mathbf{x})\mathbf{I}\big)\ell \\ &\quad \in \mathbb{S} \quad \forall p, i, j, \end{aligned} \tag{35}$$

$$-\ell^T\big(\mathbf{Q}_q - \mu_{[q,p]}\mathbf{Q}_p + \varphi_8\mathbf{I}\big)\ell \in \mathbb{S} \quad \forall q \neq p, \tag{36}$$

where ℓ *is an arbitrary vector independent of* $\mathbf{x}$ *with appropriate dimensions;* φ_1, *and* φ_8 *are predefined positive constants;* $\varphi_2(\mathbf{x})$, $\varphi_3(\mathbf{x})$, $\varphi_4(\mathbf{x})$, $\varphi_5(\mathbf{x})$, $\varphi_6(\mathbf{x})$, *and* $\varphi_7(\mathbf{x})$ *are predefined positive scalar polynomials;*

$$\tilde{\Xi}_{1pqij}(\mathbf{x}) = \begin{bmatrix} \tilde{\mathbf{Z}}_{1pqij}(\mathbf{x}) & \mathbf{C}_{pi}(\mathbf{x}) & \mathbf{Q}_q\mathbf{D}_{pi}(\mathbf{x})^T \\ * & -\gamma_p^2\mathbf{I} & \mathbf{0} \\ * & * & -\mathbf{I} \end{bmatrix}; \tag{37}$$

$$\tilde{\Xi}_{2pij}(\mathbf{x}) = \begin{bmatrix} \tilde{\mathbf{Z}}_{2pij}(\mathbf{x}) & \mathbf{C}_{pi}(\mathbf{x}) & \mathbf{Q}_p\mathbf{D}_{pi}(\mathbf{x})^T \\ * & -\gamma_p^2\mathbf{I} & \mathbf{0} \\ * & * & -\mathbf{I} \end{bmatrix}; \tag{38}$$

$\tilde{\mathbf{Z}}_{1pqij}(\mathbf{x}) = -\beta_p\mathbf{Q}_q + \mathbf{A}_{pi}(\mathbf{x})\mathbf{Q}_q + \mathbf{B}_{pi}(\mathbf{x})\mathbf{X}_{qj}(\mathbf{x}) + (\mathbf{A}_{pi}(\mathbf{x})\mathbf{Q}_q)^T + (\mathbf{B}_{pi}(\mathbf{x})\mathbf{X}_{qj}(\mathbf{x}))^T$; $\tilde{\mathbf{Z}}_{2pij}(\mathbf{x}) = \alpha_p\mathbf{Q}_p + \mathbf{A}_{pi}(\mathbf{x})\mathbf{Q}_p + \mathbf{B}_{pi}(\mathbf{x})\mathbf{X}_{pj}(\mathbf{x}) + (\mathbf{A}_{pi}(\mathbf{x})\mathbf{Q}_p)^T + (\mathbf{B}_{pi}(\mathbf{x})\mathbf{X}_{pj}(\mathbf{x}))^T$.

Then, for any switching signal with AED-ADT $\tau_{q,p}$ *(15), the asynchronously switched polynomial fuzzy systems (9)–(10) with* $\mathbf{w} \equiv 0$ *are GUAS and have a non-weighted* L_2*-gain index no greater than* γ *(16). The feedback gains in (8) are given by* $\mathbf{K}_{pj}(\mathbf{x}) = \mathbf{X}_{pj}(\mathbf{x})\mathbf{Q}_p^{-1}$.

Proof The MLFs candidate is proposed as

$$V_p(\mathbf{x}) = \mathbf{x}^T\mathbf{Q}_p^{-1}\mathbf{x}, \quad \forall\hat{\sigma}(t) = p \in \underline{N}, \tag{39}$$

where $\mathbf{Q}_p = \mathbf{Q}_p^T > 0$. The MLFs candidate is both radially unbounded and positive-definite, i.e., the condition (29) can ensure that (11) in Theorem 1 holds.

Next, denoting $\mathbf{X}_{qj}(\mathbf{x}) = \mathbf{K}_{qj}(\mathbf{x})\mathbf{Q}_q$, from (9), (10), and (12), we have

$$\begin{aligned} &\dot{V}_q(\mathbf{x}) - \beta_p V_q(\mathbf{x}) + \Gamma(t) \\ &= \dot{\mathbf{x}}^T\mathbf{Q}_q^{-1}\mathbf{x} + \mathbf{x}^T\mathbf{Q}_q^{-1}\dot{\mathbf{x}} - \beta_p\mathbf{x}^T\mathbf{Q}_q^{-1}\mathbf{x} + \Gamma(t) \\ &= \sum_{i=1}^{n_p}\sum_{j=1}^{r_q}\omega_{pi}(\mathbf{x})m_{qj}(\mathbf{x})\Big(\big((\mathbf{A}_{pi}(\mathbf{x}) + \mathbf{B}_{pi}(\mathbf{x})\mathbf{K}_{qj}(\mathbf{x}))\mathbf{x} \\ &\quad + \mathbf{C}_{pi}(\mathbf{x})\mathbf{w}\big)^T\mathbf{Q}_q^{-1}\mathbf{x} \\ &\quad + \mathbf{x}^T\mathbf{Q}_q^{-1}\big((\mathbf{A}_{pi}(\mathbf{x}) + \mathbf{B}_{pi}(\mathbf{x})\mathbf{K}_{qj}(\mathbf{x}))\mathbf{x} + \mathbf{C}_{pi}(\mathbf{x})\mathbf{w}\big) \\ &\quad - \beta_p\mathbf{x}^T\mathbf{Q}_q^{-1}\mathbf{x} \\ &\quad + \big(\mathbf{D}_{pi}(\mathbf{x})\mathbf{x}\big)^T\big(\mathbf{D}_{pi}(\mathbf{x})\mathbf{x}\big) - \gamma_p^2\mathbf{w}^T\mathbf{w}\Big) \\ &= \sum_{i=1}^{n_p}\sum_{j=1}^{r_q}\omega_{pi}(\mathbf{x})m_{qj}(\mathbf{x})\theta_q{}^T\Xi_{1pqij}\theta_q, \end{aligned} \tag{40}$$

where

$$\Xi_{1pqij}(\mathbf{x}) = \begin{bmatrix} \mathbf{A}_{pi}(\mathbf{x})\mathbf{Q}_q + \mathbf{B}_{pi}(\mathbf{x})\mathbf{X}_{qj}(\mathbf{x}) + \mathbf{Q}_q\mathbf{A}_{pi}(\mathbf{x})^T & \\ +(\mathbf{B}_{pi}(\mathbf{x})\mathbf{X}_{qj}(\mathbf{x}))^T - \beta_p\mathbf{Q}_q & \mathbf{C}_{pi}(\mathbf{x}) \\ +(\mathbf{D}_{pi}(\mathbf{x})\mathbf{Q}_q)^T\mathbf{D}_{pi}(\mathbf{x})\mathbf{Q}_q & \\ * & -\gamma_p^2\mathbf{I} \end{bmatrix}$$

$\forall q \neq p, q, p \in \underline{N}, i \in \underline{n_p}, j \in \underline{r_q}$ and $\theta_q = [(\mathbf{Q}_q^{-1}\mathbf{x})^T \quad \mathbf{w}^T]^T$.

To deal with the non-convex term $(\mathbf{D}_{pi}(\mathbf{x})\mathbf{Q}_q)^T\mathbf{D}_{pi}(\mathbf{x})\mathbf{Q}_q$, using the Schur complement, one can obtain $\tilde{\Xi}_{1pqij}(\mathbf{x})$ as represented in (37).

Considering $\underline{\gamma}_{pqij}$ as the lower bounds of $\omega_{pi}(\mathbf{x})m_{qj}(\mathbf{x})$ and $\overline{\gamma}_{pqij}$ as the upper bounds of $\omega_{pi}(\mathbf{x})m_{qj}(\mathbf{x})$, we have $\underline{\gamma}_{pqij} \leq \omega_{pi}(\mathbf{x})m_{qj}(\mathbf{x}) \leq \overline{\gamma}_{pqij}$. Further, by defining slack polynomial matrices $\overline{\mathbf{R}}_{1pqij}(\mathbf{x})$ and $\underline{\mathbf{R}}_{1pqij}(\mathbf{x})$, we can get

$$\big(\overline{\gamma}_{pqij} - \omega_{pi}(\mathbf{x})m_{qj}(\mathbf{x})\big)\overline{\mathbf{R}}_{1pqij}(\mathbf{x}) \geq 0, \tag{41}$$

$$\left(\omega_{pi}(\mathbf{x})m_{qj}(\mathbf{x}) - \underline{\gamma}_{pqij}\right)\underline{\mathbf{R}}_{1pqij}(\mathbf{x}) \geq 0. \tag{42}$$

Denoting $\zeta_q = [(\mathbf{Q}_q^{-1}\mathbf{x})^T \quad \mathbf{w}^T \quad \mathbf{I}_{\vartheta\times 1}]^T$, adding (41) and (42) to (40), we have

$$\begin{aligned}
&\dot{V}_q(\mathbf{x}) - \beta_p V_q(\mathbf{x}) + \Gamma(t) \\
&\leq \sum_{i=1}^{n_p}\sum_{j=1}^{r_q}\omega_{pi}(\mathbf{x})m_{qj}(\mathbf{x})\zeta_q{}^T\tilde{\Xi}_{1pqij}(\mathbf{x})\zeta_q \\
&\quad + \sum_{i=1}^{n_p}\sum_{j=1}^{r_q}\left(\overline{\gamma}_{pqij} - \omega_{pi}(\mathbf{x})m_{qj}(\mathbf{x})\right) \\
&\times \zeta_q{}^T\overline{\mathbf{R}}_{1pqij}(\mathbf{x})\zeta_q + \sum_{i=1}^{n_p}\sum_{j=1}^{r_q}\left(\omega_{pi}(\mathbf{x})m_{qj}(\mathbf{x}) - \underline{\gamma}_{pqij}\right) \\
&\quad \zeta_q{}^T\underline{\mathbf{R}}_{1pqij}(\mathbf{x})\zeta_q \\
&= \sum_{i=1}^{n_p}\sum_{j=1}^{r_q}\omega_{pi}(\mathbf{x})m_{qj}(\mathbf{x})\zeta_q{}^T\big(\tilde{\Xi}_{1pqij}(\mathbf{x}) \\
&\quad + \underline{\mathbf{R}}_{1pqij}(\mathbf{x}) - \overline{\mathbf{R}}_{1pqij}(\mathbf{x}) \\
&\quad + \sum_{r=1}^{n_p}\sum_{s=1}^{r_q}(\overline{\gamma}_{pqrs}\overline{\mathbf{R}}_{1pqrs}(\mathbf{x}) - \underline{\gamma}_{pqrs}\underline{\mathbf{R}}_{1pqrs}(\mathbf{x}))\big)\zeta_q.
\end{aligned} \tag{43}$$

Then, it can be seen that if (30)–(34) holds, (12) in Theorem 1 can be guaranteed.

Following similar manipulation as (40)–(43), and denoting $\mathbf{X}_{pj}(\mathbf{x}) = \mathbf{K}_{pj}(\mathbf{x})\mathbf{Q}_p$, from (9), (10), and (13), one can obtain

$$\begin{aligned}
&\dot{V}_p(\mathbf{x}) + \alpha_p V_p(\mathbf{x}) + \Gamma(t) \\
&\leq \sum_{i=1}^{n_p}\sum_{j=1}^{r_p}\omega_{pi}(\mathbf{x})m_{pj}(\mathbf{x})\zeta_p{}^T(\tilde{\Xi}_{2pij}(\mathbf{x}) + \underline{\mathbf{R}}_{2pij}(\mathbf{x}) - \overline{\mathbf{R}}_{2pij}(\mathbf{x}) \\
&\quad + \sum_{r=1}^{n_p}\sum_{s=1}^{r_p}(\overline{\gamma}_{prs}\overline{\mathbf{R}}_{2prs}(\mathbf{x}) - \underline{\gamma}_{prs}\underline{\mathbf{R}}_{2prs}(\mathbf{x})))\zeta_p,
\end{aligned} \tag{44}$$

where $\zeta_p = [(\mathbf{Q}_p^{-1}\mathbf{x})^T \quad \mathbf{w}^T \quad \mathbf{I}_{\vartheta\times 1}]^T$ and $\tilde{\Xi}_{2pij}$ is represented by (38). Thus, one can conclude that (30)–(33) and (35) guarantee (13) in Theorem 1 holds.

Moreover, from (14) and (39), we obtain

$$\begin{aligned}
&V_p(\mathbf{x}(\hat{t}_\pi)) - \mu_{[q,p]}V_q(\mathbf{x}(\hat{t}_\pi)) \\
&= \mathbf{x}(\hat{t}_\pi)^T\mathbf{Q}_p^{-1}\mathbf{x}(\hat{t}_\pi) - \mu_{[q,p]}\mathbf{x}(\hat{t}_\pi)^T\mathbf{Q}_q^{-1}\mathbf{x}(\hat{t}_\pi) \\
&= \mathbf{x}(\hat{t}_\pi)^T\left(\mathbf{Q}_p^{-1} - \mu_{[q,p]}\mathbf{Q}_q^{-1}\right)\mathbf{x}(\hat{t}_\pi).
\end{aligned} \tag{45}$$

By Schur complement, we have

$$\begin{bmatrix} -\mu_{[q,p]}\mathbf{Q}_q^{-1} & \mathbf{I} \\ * & -\mathbf{Q}_p \end{bmatrix} \leq 0. \tag{46}$$

Using Schur complement again, we can get (46) is equivalent to

$$-\mathbf{Q}_p - \mathbf{I}^T(-\mu_{[q,p]}\mathbf{Q}_q{}^{-1})^{-1}\mathbf{I} \leq 0. \tag{47}$$

Thus, one can conclude that (36) guarantees (14) in Theorem 1. □

Remark 4 The controller gains can be set as polynomial matrices rather than constant matrices in Theorem 2. When the order of controller gain is set to 0, and the slack polynomial matrices $\overline{\mathbf{R}}_{1pqij}(\mathbf{x})$, $\underline{\mathbf{R}}_{1pqij}(\mathbf{x})$ are removed, the derived conditions are consistent with the LMI-based conditions in [11] and [12]. Therefore, by setting polynomial controller gains and introducing more information of membership functions, the feasible solutions for the conditions can be obtained by tighter given constants $\mu_{[q,p]}$, β_p, α_p and γ_p in Theorem 2, which conduces to reduce the L_2-gain index.

3.3 Relaxed Conditions of Asynchronously Switched Polynomial Fuzzy Systems Based on High-Order MLFs

In the above subsection, Theorem 2 is derived from quadratic MLFs. This subsection proposes high-order MLFs to obtain tighter switching signal parameters to improve anti-interference performance. The high-order MLFs refer to the positive-definite matrices of MLFs in polynomial form. However, a challenge is how to handle the derivative of the polynomial matrices. For example, setting $V_p(\mathbf{x}) = \mathbf{x}^T\mathbf{Q}_p(\mathbf{x})\mathbf{x}$, thus, the problematic term that need to handle is $\mathbf{x}^T\dot{\mathbf{Q}}_p(\mathbf{x})\mathbf{x} = \mathbf{x}^T(\sum_{k=1}^{n}\frac{\partial\mathbf{Q}_p(\mathbf{x})}{\partial x_k}((\mathbf{A}_{pi}^k(\mathbf{x}) + \mathbf{B}_{pi}^k(\mathbf{x})\mathbf{K}_{pj}(\mathbf{x}))\mathbf{x} + \mathbf{C}_{pi}^k(\mathbf{x})\mathbf{w}))\mathbf{x}$. Here, $\mathbf{x}^T\frac{\partial\mathbf{Q}_p(\mathbf{x})}{\partial x_k}\mathbf{C}_{pi}^k(\mathbf{x})\mathbf{w}\mathbf{x}$ and $\mathbf{x}^T\frac{\partial\mathbf{Q}_p(\mathbf{x})}{\partial x_k}\mathbf{B}_{pi}^k(\mathbf{x})\mathbf{K}_{pj}(\mathbf{x})\mathbf{x}$ are non-convex terms. To tackle this problem, we introduce the concept of homogeneous polynomial function as below.

Definition 2 (*see* [29]) If a polynomial function $V(\mathbf{z}) : \Re^n \to \Re$ satisfies the identity $V(\varepsilon\mathbf{z}) = \varepsilon^d V(\mathbf{z}), \forall\varepsilon \geq 0$, then $V(\mathbf{z})$ is considered as a homogeneous polynomial function of order d.

Based on the Euler's homogeneity, $V(\mathbf{z})$ has the property

$$V(\mathbf{z}) = \frac{1}{d(d-1)}\mathbf{z}^T\nabla_{zz}V(\mathbf{z})\mathbf{z}, \tag{48}$$

where $\nabla_{zz}V(\mathbf{z}) = \begin{bmatrix} \frac{\partial^2V(\mathbf{z})}{\partial z_1^2} & \frac{\partial^2V(\mathbf{z})}{\partial z_1\partial z_2} & \cdots & \frac{\partial^2V(\mathbf{z})}{\partial z_1\partial z_n} \\ \frac{\partial^2V(\mathbf{z})}{\partial z_2\partial z_1} & \frac{\partial^2V(\mathbf{z})}{\partial z_2^2} & \cdots & \frac{\partial^2V(\mathbf{z})}{\partial z_2\partial z_n} \\ \vdots & \vdots & \ddots & \vdots \\ \frac{\partial^2V(\mathbf{z})}{\partial z_n\partial z_1} & \frac{\partial^2V(\mathbf{z})}{\partial z_n\partial z_2} & \cdots & \frac{\partial^2V(\mathbf{z})}{\partial z_n^2} \end{bmatrix}$ is the Hessian matrix. Besides, the derivative of homogeneous polynomial function $V(\mathbf{z})$ has the following property $\dot{V}(\mathbf{z}) =$

$\frac{1}{2(d-1)}(\dot{\mathbf{z}}^T \bigtriangledown_{zz} V(\mathbf{z})\mathbf{z}+\mathbf{z}^T \bigtriangledown_{zz} V(\mathbf{z})\dot{\mathbf{z}})$. By employing the property of homogeneous polynomials, the proposed high-order MLFs candidate are constructed as

$$\begin{aligned} V_p(\mathbf{x}) &= V_p^1(\mathbf{x}) + V_p^2(\mathbf{x}) + \cdots + V_p^{\varpi}(\mathbf{x}) \\ &= \mathbf{x}^T \sum_{\pi=1}^{\varpi} \frac{1}{d_\pi(d_\pi-1)} \mathbf{P}_p^\pi(\mathbf{x})\mathbf{x}, \\ &= \mathbf{x}^T \mathbf{P}_p(\mathbf{x})\mathbf{x}, \end{aligned} \tag{49}$$

where d_π is the order of $V_p^\pi(\mathbf{x})$.

Remark 5 The high-order MLFs designed in this paper comprise homogeneous polynomial functions of different orders, which can be regarded as an extension of the quadratic MLFs. More importantly, the high-order MLFs can avoid generating non-convex terms $\mathbf{x}^T\dot{\mathbf{Q}}_p(\mathbf{x})\mathbf{x}$ by using Euler's homogeneity property.

Theorem 3 *Consider the asynchronously switched polynomial fuzzy systems (9)–(10), and let $\mu_{[q,p]} > 1$, $\beta_p > 0$, $\alpha_p > 0$ and $\gamma_p > 0$ for $\forall q \neq p$, $q, p \in \underline{N}$ be given constants. Defining the symmetric polynomial matrices $\mathbf{P}_p^\pi(\mathbf{x})$, $p \in \underline{N}, \pi \in \varpi$, slack polynomial matrices $\overline{\mathbf{R}}_{3pqij}(\mathbf{x})$, $\underline{\mathbf{R}}_{3pqij}(\mathbf{x})$, $q \neq p, q, p \in \underline{N}, i \in \underline{n_p}, j \in \underline{r_q}$ and $\overline{\mathbf{R}}_{4pij}(\mathbf{x})$, $\underline{\mathbf{R}}_{4pij}(\mathbf{x})$, $p \in \underline{N}, i \in \underline{n_p}, j \in \underline{r_p}$, if there exist feasible solutions to the following conditions:*

$$\ell^T\big(\mathbf{P}_p(\mathbf{x}) - \varphi_9(\mathbf{x})\mathbf{I}\big)\ell \in \mathbb{S} \quad \forall p, \tag{50}$$

$$\ell^T\big(\overline{\mathbf{R}}_{3pqij}(\mathbf{x}) - \varphi_{10}(\mathbf{x})\mathbf{I}\big)\ell \in \mathbb{S} \quad \forall q \neq p, i, j, \tag{51}$$

$$\ell^T\big(\underline{\mathbf{R}}_{3pqij}(\mathbf{x}) - \varphi_{11}(\mathbf{x})\mathbf{I}\big)\ell \in \mathbb{S} \quad \forall q \neq p, i, j, \tag{52}$$

$$\ell^T\big(\overline{\mathbf{R}}_{4pij}(\mathbf{x}) - \varphi_{12}(\mathbf{x})\mathbf{I}\big)\ell \in \mathbb{S} \quad \forall p, i, j, \tag{53}$$

$$\ell^T\big(\underline{\mathbf{R}}_{4pij}(\mathbf{x}) - \varphi_{13}(\mathbf{x})\mathbf{I}\big)\ell \in \mathbb{S} \quad \forall p, i, j, \tag{54}$$

$$\begin{aligned} &-\ell^T\big(\Xi_{3pqij}(\mathbf{x}) + \underline{\mathbf{R}}_{3pqij}(\mathbf{x}) - \overline{\mathbf{R}}_{3pqij}(\mathbf{x}) \\ &\quad + \sum_{r=1}^{n_p}\sum_{s=1}^{r_q}(\overline{\gamma}_{pqrs}\overline{\mathbf{R}}_{3pqrs}(\mathbf{x}) \\ &\quad - \underline{\gamma}_{pqrs}\underline{\mathbf{R}}_{3pqrs}(\mathbf{x})) + \varphi_{14}(\mathbf{x})\mathbf{I}\big)\ell \in \mathbb{S} \quad \forall q \neq p, i, j, \end{aligned} \tag{55}$$

$$\begin{aligned} &-\ell^T\big(\Xi_{4pij}(\mathbf{x}) + \underline{\mathbf{R}}_{4pij}(\mathbf{x}) - \overline{\mathbf{R}}_{4pij}(\mathbf{x}) \\ &\quad + \sum_{r=1}^{n_p}\sum_{s=1}^{r_p}(\overline{\gamma}_{prs}\overline{\mathbf{R}}_{4prs}(\mathbf{x}) \\ &\quad - \underline{\gamma}_{prs}\underline{\mathbf{R}}_{4prs}(\mathbf{x})) + \varphi_{15}(\mathbf{x})\mathbf{I}\big)\ell \in \mathbb{S} \quad \forall p, i, j, \end{aligned} \tag{56}$$

$$-\ell^T\big(\mathbf{P}_p(\mathbf{x}) - \mu_{[q,p]}\mathbf{P}_q(\mathbf{x}) + \varphi_{16}(\mathbf{x})\mathbf{I}\big)\ell \in \mathbb{S} \quad \forall q \neq p, \tag{57}$$

where ℓ is an arbitrary vector independent of $\mathbf{x}$ with appropriate dimensions; $\varphi_9(\mathbf{x})$, $\varphi_{10}(\mathbf{x})$, $\varphi_{11}(\mathbf{x})$, $\varphi_{12}(\mathbf{x})$, $\varphi_{13}(\mathbf{x})$, $\varphi_{14}(\mathbf{x})$, $\varphi_{15}(\mathbf{x})$, and $\varphi_{16}(\mathbf{x})$ are predefined positive-definite scalar polynomials;

$$\Xi_{3pqij} = \begin{bmatrix} \mathbf{Z}_{3pqij} & \mathbf{C}_{pi}(\mathbf{x}) \\ * & -\gamma_p^2\mathbf{I} \end{bmatrix}, \quad \forall q \neq p, i, j; \tag{58}$$

$$\Xi_{4pqij} = \begin{bmatrix} \mathbf{Z}_{4pqij} & \mathbf{C}_{pi}(\mathbf{x}) \\ * & -\gamma_p^2\mathbf{I} \end{bmatrix}, \quad \forall q \neq p, i, j; \tag{59}$$

$\mathbf{Z}_{3pqij} = \mathbf{M}_q(\mathbf{x})\mathbf{A}_{pi}(\mathbf{x}) + \mathbf{M}_q(\mathbf{x})\mathbf{B}_{pi}(\mathbf{x})\mathbf{K}_{qj}(\mathbf{x}) + \mathbf{A}_{pi}(\mathbf{x})^T \mathbf{M}_q(\mathbf{x}) + (\mathbf{B}_{pi}(\mathbf{x})\mathbf{K}_{qj}(\mathbf{x}))^T \times\mathbf{M}_q(\mathbf{x}) - \beta_p\mathbf{P}_q(\mathbf{x}) + \mathbf{D}_{pi}(\mathbf{x})^T\mathbf{D}_{pi}(\mathbf{x})$; $\mathbf{Z}_{4pqij} = \mathbf{M}_p(\mathbf{x})\mathbf{A}_{pi}(\mathbf{x}) + \mathbf{M}_p(\mathbf{x})\mathbf{B}_{pi}(\mathbf{x})\mathbf{K}_{pj}(\mathbf{x}) + \mathbf{A}_{pi}(\mathbf{x})^T\mathbf{M}_p(\mathbf{x}) + (\mathbf{B}_{pi}(\mathbf{x})\mathbf{K}_{pj}(\mathbf{x}))^T\mathbf{M}_p(\mathbf{x}) + \alpha_p\mathbf{P}_p(\mathbf{x}) + \mathbf{D}_{pi}(\mathbf{x})^T\mathbf{D}_{pi}(\mathbf{x})$; $\mathbf{M}_p(\mathbf{x}) = \sum_{\pi=1}^{\varpi}\frac{1}{2(d_\pi-1)}\mathbf{P}_p^\pi(\mathbf{x})$ *and* $\mathbf{P}_p(\mathbf{x}) = \sum_{\pi=1}^{\varpi}\frac{1}{d_\pi(d_\pi-1)}\mathbf{P}_p^\pi(\mathbf{x})$.

Then, for any switching signal with AED-ADT $\tau_{q,p}$ (15), with the given controller $\mathbf{K}_{pj}(\mathbf{x})$, the asynchronously switched polynomial fuzzy systems (9)–(10) with $\mathbf{w} \equiv 0$ are GUAS and have a non-weighted L_2-gain index no greater than γ (16).

Proof The high-order MLFs candidate is shown in (49). When $\mathbf{P}_p(\mathbf{x}) > 0$, we can get the MLFs candidate is both radially unbounded and positive-definite. Thus, one can obtain (50) holds, which means (11) in Theorem 1 can be guaranteed.

Next, denote $\mathbf{M}_q(\mathbf{x}) = \sum_{\pi=1}^{\varpi}\frac{1}{2(d_\pi-1)}\mathbf{P}_q^\pi(\mathbf{x})$, from (9), (10), and (12), one can obtain

$$\begin{aligned} &\dot{V}_q(\mathbf{x}) - \beta_p V_q(\mathbf{x}) + \Gamma(t) \\ &= \dot{\mathbf{x}}^T\mathbf{M}_q(\mathbf{x})\mathbf{x} + \mathbf{x}^T\mathbf{M}_q(\mathbf{x})\dot{\mathbf{x}} - \beta_p\mathbf{x}^T\mathbf{P}_q(\mathbf{x})\mathbf{x} + \Gamma(t) \\ &= \sum_{i=1}^{n_p}\sum_{j=1}^{r_q}\omega_{pi}(\mathbf{x})m_{qj}(\mathbf{x})\xi_q{}^T\Xi_{3pqij}(\mathbf{x})\xi_q, \end{aligned} \tag{60}$$

where $\xi_q = [\mathbf{x}^T \quad \mathbf{w}^T]^T$ and Ξ_{3pqij} is represented in (58).

Referring to the mathematical method of introducing slack matrices $\overline{\mathbf{R}}_{1pqij}(\mathbf{x})$ and $\underline{\mathbf{R}}_{1pqij}(\mathbf{x})$ in Theorem 2, conditions (51)–(55) can be obtained, thus ensuring that (12) in Theorem 1 holds. Similarly, the process of obtaining (56) was omitted due to page limitations. Therefore, one can conclude that (51)–(54) and (56) guarantee (13) in Theorem 1 holds.

Moreover, from (14) and (49), we have

$$\begin{aligned} &V_p(\mathbf{x}(\hat{t}_\pi)) - \mu_{[q,p]}V_q(\mathbf{x}(\hat{t}_\pi)) \\ &= \mathbf{x}(\hat{t}_\pi)^T(\mathbf{P}_p(\mathbf{x}) - \mu_{[q,p]}\mathbf{P}_q(\mathbf{x}))\mathbf{x}(\hat{t}_\pi) \leq 0. \end{aligned} \tag{61}$$

Thus, condition (57) can ensure that (14) in Theorem 1 holds. □

Remark 6 The high-order MLFs based on the property of homogeneous function can deal with the problem of deriving the non-convex term $\mathbf{x}^T\dot{\mathbf{Q}}_p(\mathbf{x})\mathbf{x}$. Thus, higher order Lyapunov functions can be incorporated into the conditions to obtain the L_2-gain index. However, it is worth noting that Theorem 3 still includes bilinear terms. An algorithm is proposed to obtain the controller with a lower L_2-gain index as follows:

Algorithm: Design of the controller with a lower L_2-gain index

Input: $\mu_{[q,p]}$, α_p, β_p, γ_p and $\mathscr{T}_{\mathrm{m}}$.
Step 1: Choose $\mu_{[q,p]}$ as large as possible, e.g., $\mu_{[q,p]} > 10$. Choose α_p and β_p as small as possible, e.g., $\beta_p < 1$ and $\alpha_p < 1$. Let $\gamma_p = 1$ and $\mathscr{T}_{\mathrm{m}} = 1$ without loss of generality.
Step 2: Get the solution from the conditions (29)–(36) of Theorem 2.
Step 3: If no solution is found, terminate this algorithm. If a solution can be found, then reduce $\mu_{[q,p]}$ and increase α_p, β_p and go to step 2 until a solution cannot be found.
Step 4: With the feasible $\mu_{[q,p]}$, α_p, β_p and $\mathbf{K}_{pj}(\mathbf{x})$ obtained in Step 3, get the solution from the conditions (50)–(57) of Theorem 3.
Step 5: Reduce $\mu_{[q,p]}$ and increase α_p, β_p, go to step 4 until a solution cannot be found, then, the iteration stops. Get the smaller $\mu_{[q,p]}$ and larger α_p, β_p, and calculate the L_2-gain index γ according to (16).
Output: The controller gains $\mathbf{K}_{pj}(\mathbf{x})$ and the non-weighted L_2-gain index γ.

Remark 7 Compared to the Theorem in [11], [12], and [19], Theorem 3 is based on high-order MLFs and can search for feasible solutions on a larger scale. In addition, by utilizing the properties of homogeneous polynomial functions, it can handle the non-convex terms from the derivative of $\mathbf{P}(\mathbf{x})$, whereas the high-order MLFs in [18] cannot deal with them. The relaxed analysis results can reduce the L_2-gain index, improving the anti-disturbance capability. The comparison between the proposed and existing methods is presented in Table 2.

Table 2 Comparison between the proposed method and existing methods

References	[11]	[12]	[18]	[19]	This paper
Switched subsystem	Linear	T-S fuzzy	Polynomial fuzzy	Polynomial fuzzy	Polynomial fuzzy
System constraint	Disturbance	Disturbance	None	Positive	Disturbance
Controller constraint	Asynchrony	Asynchrony	None	None	Asynchrony
MLFs	$\mathbf{x}^T P_i^{-1}\mathbf{x}$ quadratic	$\mathbf{x}^T P_i^{-1}\mathbf{x}$ quadratic	$\mathbf{x}^T P_i(\mathbf{x})\mathbf{x}$ high-order	$v_p^T\mathbf{x}$ one-order	$\mathbf{x}^T P_i(\mathbf{x})\mathbf{x}$ high-order
Procedure	None	None	Constrainted two-step	None	Two-step
Conditions	LMI	LMI	SOS	SOS	SOS
MFD	None	None	Approximate	Approximate	Boundary
Stable region	Global	Global	Local	Local	Global
Concern	L_2-gain	L_2-gain	Stability	Positive	L_2-gain

4 Simulation Example

In this section, we provide two simulation examples to validate the advantages of the developed approach.

4.1 Asynchronously Switched Polynomial Fuzzy Systems

In the simulation example, we set three scenarios to validate the advantages of the developed approach.

(1) The difference between the switched polynomial fuzzy model and switched T-S fuzzy model.

(2) The difference between the non-weighted L_2-gain based on AED-ADT switching signal and the results in [12] based on MDADT switching signal.
(3) The effect of membership function information and high-order MLFs on the stability results and non-weighted L_2-gain performance index of asynchronously switched polynomial fuzzy systems.

Consider an asynchronously switched polynomial fuzzy system with three subsystems, as shown below.

$$\mathbf{A}_{11}(x_1)=\begin{bmatrix}-0.2-0.2x_1^2 & 0.5\\ 0.1 & -1+0.2x_1^2\end{bmatrix},$$
$$\mathbf{A}_{12}(x_1)=\begin{bmatrix}-0.1-0.6x_1^2 & 0.2\\ 0.2 & -0.5+0.3x_1^2\end{bmatrix},$$
$$\mathbf{B}_{11}=\begin{bmatrix}1\\2\end{bmatrix},\mathbf{B}_{12}=\begin{bmatrix}2\\4\end{bmatrix},\mathbf{C}_{11}=\begin{bmatrix}0.2\\0.1\end{bmatrix},\mathbf{C}_{12}=\begin{bmatrix}0.5\\0.2\end{bmatrix},$$
$$\mathbf{D}_{11}=[0.2,\ 0.2],\mathbf{D}_{12}=[0.1,\ 0.3],$$
$$\mathbf{A}_{21}(x_1)=\begin{bmatrix}0.2-0.2x_1^2 & -0.8\\ 0.5 & 1+0.2x_1^2\end{bmatrix},$$
$$\mathbf{A}_{22}(x_1)=\begin{bmatrix}0.4-0.2x_1^2 & -1.2\\ 0.6 & 1.5+0.4x_1^2\end{bmatrix},$$
$$\mathbf{B}_{21}=\begin{bmatrix}2\\1\end{bmatrix},\mathbf{B}_{22}=\begin{bmatrix}3\\2\end{bmatrix},\mathbf{C}_{21}=\begin{bmatrix}0.5\\1\end{bmatrix},\mathbf{C}_{22}=\begin{bmatrix}1\\1.2\end{bmatrix},$$
$$\mathbf{D}_{21}=[-0.1,\ 0.2],\mathbf{D}_{22}=[-0.2,\ 0.2],$$
$$\mathbf{A}_{31}(x_1)=\begin{bmatrix}0.2-0.4x_1^2 & -1\\ 1.2 & 1+0.2x_1^2\end{bmatrix},$$
$$\mathbf{A}_{32}(x_1)=\begin{bmatrix}0.3-0.2x_1^2 & -1\\ 1.5 & 2+0.1x_1^2\end{bmatrix},$$
$$\mathbf{B}_{31}=\begin{bmatrix}1\\1.6\end{bmatrix},\mathbf{B}_{32}=\begin{bmatrix}1\\1.6\end{bmatrix},\mathbf{C}_{31}=\begin{bmatrix}0.5\\1\end{bmatrix},\mathbf{C}_{32}=\begin{bmatrix}0.5\\1.6\end{bmatrix},$$
$$\mathbf{D}_{31}=[0.2,\ 0.4],\mathbf{D}_{32}=[0.2,\ 0.2].$$

We select the membership functions of the switched polynomial fuzzy systems as $\omega_{11}(x_1)=\omega_{21}(x_1)=\omega_{31}(x_1)=\frac{1}{(1+e^{x_1})e^{-x_1^2/10}}$ and $\omega_{12}(x_1)=\omega_{22}(x_1)=\omega_{32}(x_1)=1-\frac{1}{(1+e^{x_1})e^{-x_1^2/10}}$. According to the IPM design concept, we set the membership functions of the controller as $m_{11}(x_1)=m_{21}(x_1)=m_{31}(x_1)=1$.

For the first scenario, it should be pointed out that when transferring a switched polynomial fuzzy model into a switched T-S fuzzy model, it is necessary to assume in advance the operating domain of the system state, for example, $x_1\in[-c,c]$. For the nonlinear term x_1^2 in the switched polynomial fuzzy model, by using sector nonlinearity technique, it can be obtained that the switched subsystem 1 as follows:

$$\mathbf{A}_{11}(x_1)=\begin{bmatrix}-0.2 & 0.5\\ 0.1 & -1\end{bmatrix},$$
$$\mathbf{A}_{12}(x_1)=\begin{bmatrix}-0.2-0.2c^2 & 0.5\\ 0.1 & -1+0.2c^2\end{bmatrix},$$

Table 3 Comparison of different stability criteria

Case	Criteria	Switching signal
1	Theorem 2 in [12]	MDADT
2	Theorem 2 in this paper	AED-ADT

$$\mathbf{A}_{13}(x_1)=\begin{bmatrix}-0.1 & 0.2\\ 0.2 & -0.5\end{bmatrix},$$
$$\mathbf{A}_{14}(x_1)=\begin{bmatrix}-0.1-0.6c^2 & 0.2\\ 0.2 & -0.5+0.3c^2\end{bmatrix},$$

stop

$$\mathbf{B}_{11}(x_1)=\mathbf{B}_{12}(x_1)=\begin{bmatrix}1\\2\end{bmatrix},\mathbf{B}_{13}(x_1)=\mathbf{B}_{14}(x_1)=\begin{bmatrix}2\\4\end{bmatrix},$$
$$\mathbf{C}_{11}(x_1)=\mathbf{C}_{12}(x_1)=\begin{bmatrix}0.2\\0.1\end{bmatrix},\mathbf{C}_{13}(x_1)=\mathbf{C}_{14}(x_1)=\begin{bmatrix}0.5\\0.2\end{bmatrix},$$
$$\mathbf{D}_{11}=\mathbf{D}_{12}=[0.2\quad 0.2],\mathbf{D}_{13}=\mathbf{D}_{14}=[0.1\quad 0.3].$$

Switched T-S fuzzy subsystems 2 and 3 are similar to subsystem 1, omitted here due to page limitations. Set $\mathscr{T}_{\mathrm{m}}=1,\gamma_p=1,\beta_p=0.7,p\in\{1,2,3\},\varphi_1=\varphi_2(\mathbf{x})=\varphi_3(\mathbf{x})=\varphi_4(\mathbf{x})=\varphi_5(\mathbf{x})=\varphi_6(\mathbf{x})=\varphi_7(\mathbf{x})=\varphi_8=1\times10^{-3}$, $\mathbf{Q}_p(\mathbf{x})$ as constant matrices. Further, for the polynomial matrices $\mathbf{X}_{pj}(\mathbf{x})$, we set their order as 0 and 2 in x_1. For the polynomial matrices $\underline{\mathbf{R}}_{1pqij}(\mathbf{x}),\overline{\mathbf{R}}_{1pqij}(\mathbf{x}),\underline{\mathbf{R}}_{2pij}(\mathbf{x})$ and $\overline{\mathbf{R}}_{2pij}(\mathbf{x})$, we set their order as 2 in x_1. By using the Theorem 2, we only get $c=3.2$, which means the switched T-S fuzzy systems is only stable in the operating domain of $\{x_1|-3.2\le x_1\le 3.2\}$. In addition, it can be seen that the number of fuzzy rules for switched polynomial fuzzy models is 6, and the number of fuzzy rules for switched T-S fuzzy models is 12. This result indicates the advantage of switched polynomial fuzzy systems, which is the ability to ensure global stability and decrease the number of fuzzy rules.

For the second scenario, we make Table 3 to study the difference between the non-weighted L_2-gain based on AED-ADT and MDADT switching signal.

For case 1, the LMI toolbox was used in [12] to solve the conditions, thus, the controller gains can only be set as constant matrices. However, feasible solutions cannot be obtained. To make a fair comparison, we use the SOSTOOLs toolbox to solve the conditions in [12], and set the controller gains to polynomial matrices. Besides, we set the same condition parameters as in the first scenario. The upper and lower boundary values of membership functions $\omega_{pi}(\mathbf{x})m_{qj}(\mathbf{x})$ are $\overline{\gamma}_{pq11}=0.6655$, $\overline{\gamma}_{pq21}=1$, $\underline{\gamma}_{pq11}=0$ and $\underline{\gamma}_{pq21}=0.3345$ for $q\neq p,q,p\in\{1,2,3\}$. Meanwhile, the upper and lower boundary values of membership functions $\omega_{pi}(\mathbf{x})m_{pj}(\mathbf{x})$ are $\overline{\gamma}_{p11}=0.6655,\overline{\gamma}_{p21}=1,\underline{\gamma}_{p11}=0$ and $\underline{\gamma}_{p21}=0.3345$ for $\forall p=\{1,2,3\}$. By utilizing the con-

Table 4 Bounds on dwell time and controllers gains under different cases

Case	Bounds on dwell time and controller gains
1	$\mu_1 = 3.8$; $\mu_2 = 3.2$; $\mu_3 = 4.0$; $\alpha_1 \leq 0.4$; $\alpha_2 \leq 1.7$; $\alpha_3 \leq 1.9$; $\tau_1^* = 6.0875$; $\tau_2^* = 2.0960$; $\tau_3^* = 2.0980$; $\mathbf{K}_{11}(x_1) = [-0.3x_1^2 - 0.79, -2.5x_1^2 - 6.6]$; $\mathbf{K}_{21}(x_1) = [0.85x_1^2 + 1.9, -4.7x_1^2 - 13.0]$; $\mathbf{K}_{31}(x_1) = [0.7x_1^2 + 4.3, -2.6x_1^2 - 18.0]$.
2	$\mu_{[3,1]} = 3.0$; $\mu_{[2,1]} = 2.9$; $\mu_{[3,2]} = 1.6$; $\mu_{[1,2]} = 3.2$; $\mu_{[2,3]} = 1.9$; $\mu_{[1,3]} = 4.0$; $\alpha_1 \leq 0.4$; $\alpha_2 \leq 1.7$; $\alpha_3 \leq 1.9$; $\tau_{3,1}^* = 5.4965$; $\tau_{2,1}^* = 5.4118$; $\tau_{3,2}^* = 1.6882$; $\tau_{1,2}^* = 2.0960$; $\tau_{2,3}^* = 1.7062$; $\tau_{1,3}^* = 2.0980$; $\mathbf{K}_{11}(x_1) = [-0.25x_1^2 - 0.61, -2.1x_1^2 - 5.3]$; $\mathbf{K}_{21}(x_1) = [0.64x_1^2 + 1.3, -3.4x_1^2 - 9.4]$; $\mathbf{K}_{31}(x_1) = [0.58x_1^2 + 3.6, -2.3x_1^2 - 16.0]$.

ditions in [12] and this paper, Table 4 shows the obtained bounds on dwell time and controller gains.

From Table 4, one can see that the bounds on the AED-ADT switching signal are lower than those on the MDADT switching signal, meaning a more general set of admissible switching signal is obtained in this paper than the results in [12]. To verify these results, assuming one possible switching signal is periodic, such as, $\sigma(t) \in \{1 \to 2 \to 3 \to 1 \to 2 \to 3 \to \cdots\}$. For fair comparison, we set the same specific implementation switching signal for case 1 and case 2, which is $\tau_1 = \tau_{3,1} = 6.1875$, $\tau_2 = \tau_{1,2} = 2.1960$ and $\tau_3 = \tau_{2,3} = 2.1980$. The asynchronous delay is $\tau_\pi = 1, \forall \pi \in \mathbb{Z}^+$. Setting $\sum_{p=1}^{3} N_p^0 = 1$ (specifically, $N_3^0 = 1$) and $\sum_{p=1}^{3}\sum_{q\neq p,q=1}^{3} N_{q,p}^0 = 1$ (specifically, $N_{3,1}^0 = 1$), by (16) in Theorem 1, the non-weighted L_2-gain under MDADT switching signal and AED-ADT switching signal are $\gamma_{mda} = 15.84$ and $\gamma = 6.35$, respectively. This indicates that the non-weighted L_2-gain based on the AED-ADT switching signal is smaller compared to that based on the MDADT switching signal.

In fact, the AED-ADT switching signal can be selected smaller, for example, $\tau_{3,1} = 5.5965$, $\tau_{1,2} = 2.1960$, and $\tau_{2,3} = 2.7062$. With the given switching signal, the asynchronously switched polynomial fuzzy system with $w(t) \equiv 0$ is GUAS, shown in Fig. 4. Further, consider an external disturbance $w(t) = 0.5\cos(2\pi t)e^{-0.5t}$, the disturbance and system output of asynchronously switched systems are shown in Fig. 5. However, the approaches in [12] cannot guarantee the corresponding analysis results under the same switching signal.

For the third scenario, we make Table 5 to illustrate the effect of boundary information of membership functions and polynomial MLFs on the stability and non-weighted L_2-gain analysis results.

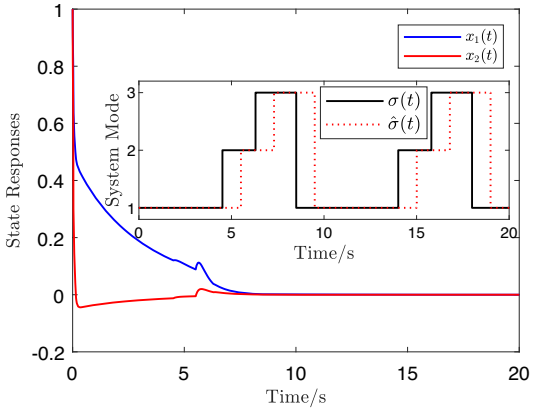

Fig. 4 The state response of asynchronous switched polynomial fuzzy system with AED-ADT switching signal and initial point [1, 1]

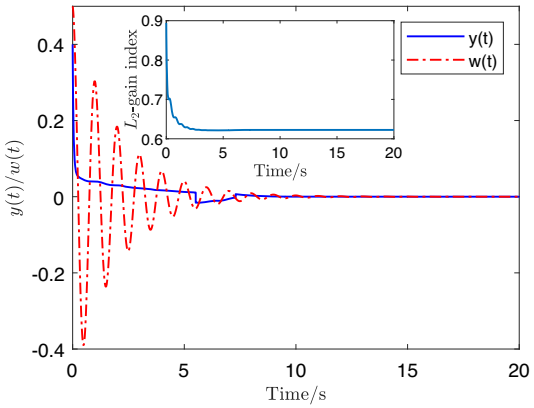

Fig. 5 Disturbance and system output of asynchronously switched polynomial fuzzy systems with the AED-ADT switching signal

Table 5 Different Settings of polynomial MLFs and boundary of membership functions

Case	Theorem	Order	Boundary Information
3	2	2	none
4	2	2	$\underline{\gamma}_{pqij}\ \overline{\gamma}_{pqij}\ \underline{\gamma}_{pij}\ \overline{\gamma}_{pij}$
5	3	4	none
6	3	4	$\underline{\gamma}_{pqij}\ \overline{\gamma}_{pqij}\ \underline{\gamma}_{pij}\ \overline{\gamma}_{pij}$

For the polynomial MLFs of order 4, we set $\mathbf{P}_p^1(\mathbf{x})$ as matrices of order 0 and $\mathbf{P}_p^2(\mathbf{x})$ as matrices of order 2. The other matrices and parameters are set the same as in the second scenario for a fair comparison of cases 3-6. By utilizing Theorem 2 and Theorem 3, Table 6 shows the obtained bounds on dwell time and non-weighted L_2-gain performance index.

From Table 6, the bounds on AED-ADT decrease with the increase of the order of polynomial MLFs and the introduction of membership function information, indicating that the conservativeness of analysis results is correspondingly reduced. The implemented AED-ADT switching signal is

Table 6 Bounds on dwell time and non-weighted L_2-gain under different cases

Case	Index	Bounds on dwell time
3	8.01	$\mu_{[3,1]} = 3.8$; $\mu_{[2,1]} = 3.8$; $\mu_{[3,2]} = 1.8$; $\mu_{[1,2]} = 3.2$; $\mu_{[2,3]} = 2.3$; $\mu_{[1,3]} = 4.0$; $\alpha_1 \leq 0.4$; $\alpha_2 \leq 1.7$; $\alpha_3 \leq 1.9$; $\tau^*_{3,1} = 6.0875$; $\tau^*_{2,1} = 6.0875$; $\tau^*_{3,2} = 1.7575$; $\tau^*_{1,2} = 2.0960$; $\tau^*_{2,3} = 1.8068$; $\tau^*_{1,3} = 2.0980$.
	6.35	$\mu_{[3,1]} = 3.0$; $\mu_{[2,1]} = 2.9$; $\mu_{[3,2]} = 1.6$; $\mu_{[1,2]} = 3.2$; $\mu_{[2,3]} = 1.9$; $\mu_{[1,3]} = 4.0$; $\alpha_1 \leq 0.4$; $\alpha_2 \leq 1.7$; $\alpha_3 \leq 1.9$; $\tau^*_{3,1} = 5.4965$; $\tau^*_{2,1} = 5.4118$; $\tau^*_{3,2} = 1.6882$; $\tau^*_{1,2} = 2.0960$; $\tau^*_{2,3} = 1.7062$; $\tau^*_{1,3} = 2.0980$.
5	4.97	$\mu_{[3,1]} = 2.2$; $\mu_{[2,1]} = 2.4$; $\mu_{[3,2]} = 1.4$; $\mu_{[1,2]} = 3.0$; $\mu_{[2,3]} = 1.9$; $\mu_{[1,3]} = 3.7$; $\alpha_1 \leq 0.4$; $\alpha_2 \leq 1.9$; $\alpha_3 \leq 2.2$; $\tau^*_{3,1} = 4.7211$; $\tau^*_{2,1} = 4.9387$; $\tau^*_{3,2} = 1.5455$; $\tau^*_{1,2} = 1.9466$; $\tau^*_{2,3} = 1.6099$; $\tau^*_{1,3} = 1.9129$.
6	4.74	$\mu_{[3,1]} = 2.0$; $\mu_{[2,1]} = 2.4$; $\mu_{[3,2]} = 1.4$; $\mu_{[1,2]} = 3.0$; $\mu_{[2,3]} = 1.9$; $\mu_{[1,3]} = 3.6$; $\alpha_1 \leq 0.4$; $\alpha_2 \leq 1.9$; $\alpha_3 \leq 2.2$; $\tau^*_{3,1} = 4.4829$; $\tau^*_{2,1} = 4.9387$; $\tau^*_{3,2} = 1.5455$; $\tau^*_{1,2} = 1.9466$; $\tau^*_{2,3} = 1.6099$; $\tau^*_{1,3} = 1.9004$.

selected as $\tau_{3,1} = 6.1875$, $\tau_{1,2} = 2.1960$, and $\tau_{2,3} = 1.9068$. The asynchronous delay is $\tau_\pi = 1, \forall \pi \in \mathbb{Z}^+$. Setting $\sum_{p=1}^{3}\sum_{q\neq p,q=1}^{3} N^0_{q,p} = 1$ (specifically, $N^0_{3,1} = 1$) for all cases, by (16) in Theorem 1, the non-weighted L_2-gain performance index is shown in Table 6. We can get that the L_2-gain index of case 6 is the smallest among all cases for the same given AED-ADT switching signal.

Furthermore, we selected the bounds on the dwell time of case 4 and case 6 of Table 6 as the switching signals. It should be pointed out that as mentioned in Remark 6, the controller feedback gains $\mathbf{K}_{pj}(\mathbf{x})$ need to be given in advance in Theorem 3. To ensure a fair comparison, the corresponding controller in Theorem 3 is obtained from Theorem 2. The system state response based on the provided AED-ADT switching signal and controllers is shown in Fig. 6.

From Fig. 6, one can observe that the amplitude fluctuation of the system state response obtained from Theorem 3 is smaller than that obtained from Theorem 2, which will provide designers with greater flexibility and space to improve system performance. Therefore, as the order of the polynomial MFLs increases and the membership function information is incorporated, it can decrease the non-weighted L_2-gain index and improve anti-disturbance performance.

In addition, we check the attenuation of polynomial MLFs to further verify the results. The positive-definite matrices of case 6 can be obtained by Theorem 3 as

$$\mathbf{P}_1(x_1) = 10^3 \times \begin{bmatrix} 0.38x_1^2 + 0.58 & -0.03x_1^2 + 4.70 \\ -0.03x_1^2 + 4.70 & 2.10x_1^2 + 3.90 \end{bmatrix},$$

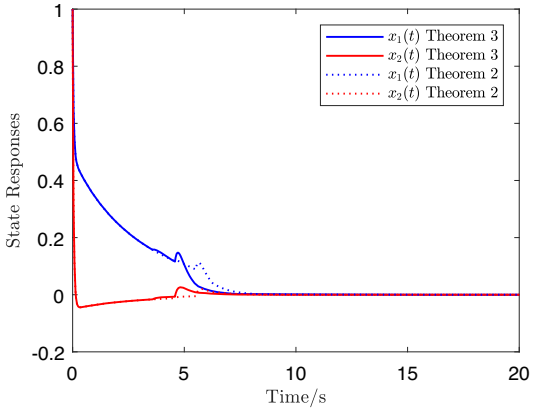

Fig. 6 State response of asynchronously switched polynomial fuzzy systems by using Theorems 2 and 3 for the same initial points [1, 1]

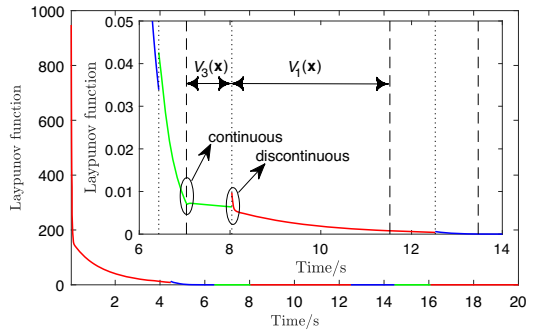

Fig. 7 The multiple Lyapunov functions with a zoomed detail around the interval [6,14]

$$\mathbf{P}_2(x_1) = 10^3 \times \begin{bmatrix} 0.49x_1^2 + 0.71 & -0.87x_1^2 - 1.80 \\ -0.87x_1^2 - 1.80 & 3.00x_1^2 + 8.40 \end{bmatrix},$$

$$\mathbf{P}_3(x_1) = 10^3 \times \begin{bmatrix} 0.58x_1^2 + 1.20 & -1.00x_1^2 - 2.40 \\ -1.00x_1^2 - 2.40 & 3.10x_1^2 + 7.70 \end{bmatrix}.$$

We set the switching sequence of the controller as $\hat{\sigma}(t) = \{4.48, 6.42, 8.04, 12.52, 14.47, 16.08, \cdots\}$ and the switching sequence of the subsystem as $\sigma(t) = \hat{\sigma}(t) - 1$. The obtained multiple Lyapunov functions candidate is shown in Fig. 7.

From Fig. 7, we can get that the MLFs approach 0 as $t \to \infty$. Meanwhile, from the zoomed details around the interval [6, 14], it can be seen that the MLFs candidate is continuous at the switching instant of the polynomial fuzzy model and discontinuous at the controller switching instant, which is consistent with the setting of the MLFs in Theorem 1. Based on the above results, the designed MLFs candidate that relies on the switching signal of the controller is capable of guaranteeing that the switched polynomial fuzzy system is GUAS with a non-weighted L_2-gain performance index.

Table 7 Different modes of parameters M and J

Mode	Parameter M	Parameter J
1	1	1
2	1.5	2
3	2	2.5

4.2 Single-Link Robot Arm System

A practical single-link robot arm system in [30] is studied using the proposed technique. The dynamics of single-link robot arm system is described by

$$\ddot{\psi}(t) = -\frac{MgL}{J}\sin(\psi(t)) - \frac{D(\psi(t))}{J}\dot{\psi}(t) + \frac{1}{J}u(t) + \frac{1}{J}w(t), \tag{62}$$

where M is the mass; J is the moment of inertia. L is the length of the arm; g is the acceleration of gravity; $\psi(t)$ is the angle position of the arm; $\dot{\psi}(t)$ is the angular velocity; $D(\psi(t)) = c_0 + c_1\psi(t)^2$ is the coefficient of viscous friction; $u(t)$ is the control input; $w(t)$ is the external disturbance. Herein, we set $g = 9.81$, $L = 0.5$, $c_0 = 2$, $c_1 = 1.1$. Besides, M and J are set according to the three different modes in the table below.

Denoting ψ, $\dot{\psi}$ as x_1, x_2, respectively, we have $\mathbf{x} = [x_1, x_2]^T$ and the state-space form of the single-link robot arm system as follows:

$$\dot{x}_1 = x_2, \tag{63}$$

$$\dot{x}_2 = -\frac{M_\sigma gL}{J_\sigma}\sin(x_1) - \frac{c_0 + c_1x_1^2}{J_\sigma}x_2 + \frac{1}{J_\sigma}u + \frac{1}{J_\sigma}w, \tag{64}$$

where $\sigma \in \{1, 2, 3\}$.

Considering that the system is working in $x_1 \in [-179.4270^\circ \quad 179.4270^\circ]$. For the nonlinear term $sin(x_1)$ in the switched first mode, we have $sin(x_1) = \mu_{L_{11}^1}(x_1)x_1 + \mu_{L_{12}^1}(x_1)\varepsilon x_1$, where $\varepsilon = 0.01/\pi$, $\mu_{L_{11}^1}(x_1) \geq 0$, $\mu_{L_{12}^1}(x_1) \geq 0$, and $\mu_{L_{11}^1}(x_1) + \mu_{L_{12}^1}(x_1) = 1$. The dynamics of single-link robot arm system can be described by a 2-rule polynomial fuzzy model as below:

Rule R_1^1: IF x_1 is about 0°, THEN

$$\dot{\mathbf{x}} = \mathbf{A}_{11}(x_1)\mathbf{x} + \mathbf{B}_{11}\mathbf{u} + \mathbf{C}_{11}w,$$
$$\mathbf{y} = \mathbf{D}_{11}\mathbf{x}.$$

Rule R_1^2: IF x_1 is about $\pm\pi$, THEN

$$\dot{\mathbf{x}} = \mathbf{A}_{12}(x_1)\mathbf{x} + \mathbf{B}_{12}\mathbf{u} + \mathbf{C}_{12}w,$$
$$\mathbf{y} = \mathbf{D}_{12}\mathbf{x}.$$

$$\mathbf{A}_{11}(x_1) = \begin{bmatrix} 0 & 1 \\ -4.9 & -2 - 1.1x_1^2 \end{bmatrix},$$
$$\mathbf{A}_{12}(x_1) = \begin{bmatrix} 0 & 1 \\ -0.016 & -2 - 1.1x_1^2 \end{bmatrix},$$
$$\mathbf{B}_{11}(x_1) = \mathbf{B}_{12}(x_1) = \mathbf{C}_{11}(x_1) = \mathbf{C}_{12}(x_1) = \begin{bmatrix} 0 \\ 1 \end{bmatrix},$$
$$\mathbf{D}_{11} = [1 \quad 0], \mathbf{D}_{12} = [1 \quad 0].$$

Similarly, the switched subsystem 2 and subsystem 3 can be represented as follows.

$$\mathbf{A}_{21}(x_1) = \begin{bmatrix} 0 & 1 \\ -3.7 & -1 - 0.6x_1^2 \end{bmatrix},$$
$$\mathbf{A}_{22}(x_1) = \begin{bmatrix} 0 & 1 \\ -0.012 & -1 - 0.6x_1^2 \end{bmatrix},$$
$$\mathbf{B}_{21}(x_1) = \mathbf{B}_{22}(x_1) = \mathbf{C}_{21}(x_1) = \mathbf{C}_{22}(x_1) = \begin{bmatrix} 0 \\ 0.5 \end{bmatrix},$$
$$\mathbf{D}_{21} = [1 \quad 0], \mathbf{D}_{22} = [1 \quad 0],$$
$$\mathbf{A}_{31}(x_1) = \begin{bmatrix} 0 & 1 \\ -3.9 & -0.8 - 0.4x_1^2 \end{bmatrix},$$
$$\mathbf{A}_{32}(x_1) = \begin{bmatrix} 0 & 1 \\ -0.012 & -0.8 - 0.4x_1^2 \end{bmatrix},$$
$$\mathbf{B}_{31}(x_1) = \mathbf{B}_{32}(x_1) = \mathbf{C}_{31}(x_1) = \mathbf{C}_{32}(x_1) = \begin{bmatrix} 0 \\ 0.4 \end{bmatrix},$$
$$\mathbf{D}_{31} = [1 \quad 0], \mathbf{D}_{32} = [1 \quad 0].$$

The membership functions of single-link robot arm system are $w_{11}(x_1) = w_{21}(x_1) = w_{31}(x_1) = \begin{cases} \frac{sin(x_1) - \varepsilon x_1}{x_1(1-\varepsilon)}, & x_1 \neq 0 \\ 1, & x_1 = 0 \end{cases}$ and $w_{12}(x_1) = w_{22}(x_1) = w_{32}(x_1)1 - w_{11}(x_1)$.

Next, choose $\varphi_1 = \varphi_2(\mathbf{x}) = \varphi_3(\mathbf{x}) = \varphi_4(\mathbf{x}) = \varphi_5(\mathbf{x}) = \varphi_6(\mathbf{x}) = \varphi_7(\mathbf{x}) = \varphi_8 = 1 \times 10^{-3}$, $\mathbf{Q}_p(\mathbf{x})$ as constant matrices. For the polynomial matrices $\mathbf{X}_{pj}(\mathbf{x})$, we set their order as 0 and 2 in x_1. For the polynomial matrices $\underline{\mathbf{R}}_{1pqij}(\mathbf{x})$, $\overline{\mathbf{R}}_{1pqij}(\mathbf{x})$, $\underline{\mathbf{R}}_{2pij}(\mathbf{x})$, and $\overline{\mathbf{R}}_{2pij}(\mathbf{x})$, we set their order as 0, 2, and 4 in x_1. By utilizing the Theorem 2, the obtained controllers are $\mathbf{K}_{11}(x_1) = [-61.0x_1^2 - 344.0, -7.9x_1^2 - 45.0]$; $\mathbf{K}_{21}(x_1) = [-56.0x_1^2 - 244.0, -7.8x_1^2 - 36.0]$; $\mathbf{K}_{31}(x_1) = [-49.0x_1^2 - 211.0, -7.1x_1^2 - 36.0]$. The following table shows the bounds on dwell time by different theorems.

To verify the results, we select the bounds on dwell time as the switching signal and set asynchronous delay $\tau_\pi = 0.1$. The system state response by using Theorem 2 and Theorem 3 is shown in Fig. 8.

Further, consider an external disturbance $w(t) = 0.5\cos(2\pi t)e^{-0.5t}$, the disturbance and system output of single-link arm system are shown in Fig. 9.

From Figs. 8 and 9, it can be seen that the single-link robot arm system can be described using such a switched

Table 8 Bounds on dwell time and non-weighted L_2-gain under different theorems

Theorem	L_2-gain	Bounds on dwell time
Theorem 2 in [12]	none	none
Theorem 2	8.5	$\mu_{[3,1]} = 3.0$; $\mu_{[2,1]} = 3.0$; $\mu_{[3,2]} = 2.0$; $\mu_{[1,2]} = 2.0$; $\mu_{[2,3]} = 1.5$; $\mu_{[1,3]} = 1.5$; $\alpha_1 \leq 9$; $\alpha_2 \leq 9$; $\alpha_3 \leq 10$; $\tau^*_{3,1} = 0.2332$; $\tau^*_{2,1} = 0.2332$; $\tau^*_{3,2} = 0.1881$; $\tau^*_{1,2} = 0.1881$; $\tau^*_{2,3} = 0.1505$; $\tau^*_{1,3} = 0.1505$.
Theorem 3	6.1	$\mu_{[3,1]} = 1.1$; $\mu_{[2,1]} = 1.1$; $\mu_{[3,2]} = 1.3$; $\mu_{[1,2]} = 1.3$; $\mu_{[2,3]} = 1.2$; $\mu_{[1,3]} = 1.2$; $\alpha_1 \leq 17$; $\alpha_2 \leq 18$; $\alpha_3 \leq 14$; $\tau^*_{3,1} = 0.1115$; $\tau^*_{2,1} = 0.1115$; $\tau^*_{3,2} = 0.1201$; $\tau^*_{1,2} = 0.1201$; $\tau^*_{2,3} = 0.1202$; $\tau^*_{1,3} = 0.1202$.

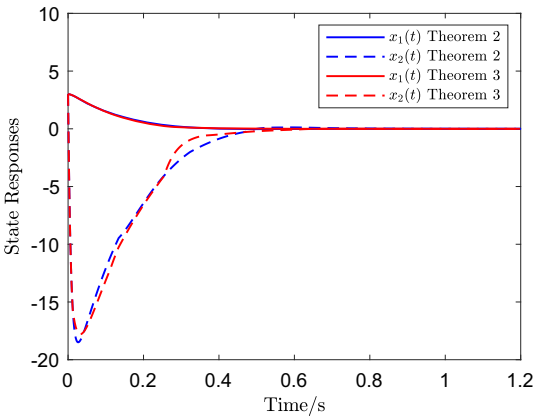

Fig. 8 State response of single-link robot arm system by using Theorem 2 and Theorem 3 for the same initial points [3, 3]

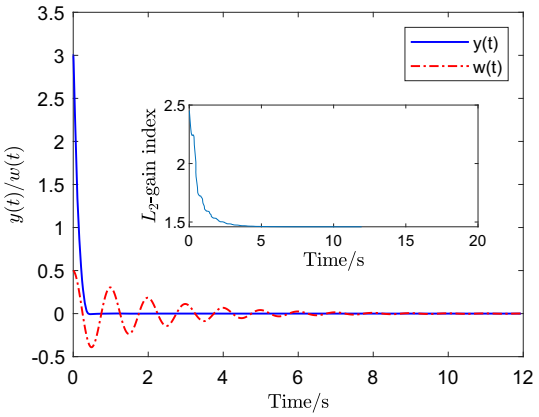

Fig. 9 Disturbance and system output of single-link robot arm system

polynomial fuzzy model and achieve stability and L_2-gain analysis.

5 Conclusion

This paper investigates the stability and L_2-gain analysis of the asynchronously switched systems described by polynomial fuzzy models. To achieve the stability and non-weighted L_2-gain performance of asynchronously switched systems, stability criteria based on AED-ADT switching signal is proposed, which can achieve a more general anti-disturbance performance compared to existing results based on ADT and MDADT. For the switched polynomial fuzzy systems, the SOS-based stability and L_2-gain conditions are obtained by utilizing the boundary information of membership functions and novel high-order MLFs, which is helpful in achieving less conservative results compared with the conventional LMI-based conditions. Finally, the effectiveness of developed approaches was demonstrated through two simulation examples. In future works, the optimization algorithms can be further studied to reduce the constraints of conditions brought by the high-order MLFs. Moreover, output-feedback and observer-based feedback controllers can be designed for more practical switched systems.

Acknowledgements This work was founded in part by Science and Technology Project of Hebei Education Department BJK2022040, Natural Science Foundation 62103356, Natural Science Foundation of Hebei Province F2021203069, Oversea Talents of Hebei Province Foundation C20210319, and Science and Technology Foundation of Qinhuangdao 202301A295, and in part by King's College London.

Data Availability The authors declare that data supporting the findings of this study are available within the article, and the figures are concrete expressions.

Declarations

Conflict of interest The authors declare that they have no known Conflict of interest or personal relationships that could have appeared to influence the work reported in this paper.

References

1. Savino, H.J., Dos Santos, C.R.P., Souza, F.O., Pimenta, L.C.A., De Oliveira, M., Palhares, R.M.: Conditions for consensus of multi-agent systems with time-delays and uncertain switching topology. IEEE Trans. Ind. Electron. **63**(2), 1258–1267 (2016)
2. Wang, X., Zhao, J.: Autonomous switched control of load shifting robot manipulators. IEEE Trans. Ind. Electron. **64**(9), 7161–7170 (2017)
3. Xiang, W., Kanjian, Z., Ming, C.: Optimal control of constrained switched systems and application to electrical vehicle energy management. Nonlinear Anal. Hybrid Syst. **30**, 171–188 (2018)
4. Zhao, X., Kao, Y., Niu, B., Wu, T.: Control Synthesis of Switched Systems. Springer, Berlin (2017)
5. Zhai, G., Lin, H., Kim, Y., Imae, J., Kobayashi, T.: L_2 gain analysis for switched systems with continuous-time and discrete-time subsystems. Int. J. Control **78**(15), 1198–1205 (2006)
6. Liu, L., Zhao, X., Sun, X., Zong, G.: Stability and l_2-gain analysis of discrete-time switched systems with mode-dependent average dwell time. IEEE Trans. Syst. Man Cybern. **50**(6), 2305–2314 (2020)
7. Ma, G., Pagilla, P.R.: Periodic event-triggered dynamic output feedback control of switched systems. Nonlinear Anal. Hybrid Syst. **31**, 247–264 (2019)
8. Zhang, L., Zhuang, S., Shi, P.: Non-weighted quasi-time-dependent H_∞ filtering for switched linear systems with persistent dwell-time. Automatica **54**, 201–209 (2015)
9. Ren, H., Zong, G., Li, T.: Event-triggered finite-time control for networked switched linear systems with asynchronous switching. IEEE Trans. Syst. Man Cybern. **48**(11), 1874–1884 (2018)
10. Qi, Q., Yang, X., Xu, Z., Zhang, M., Huang, T.: Novel LKF method on h_∞ synchronization of switched time-delay systems. IEEE Trans. Cybern. **53**(7), 4545–4554 (2023)
11. Liu, Y., Chen, X., Lu, J., Gui, W.: Non-weighted l_2/L_2-gain of asynchronously switched systems. Nonlinear Anal. Hybrid Syst. **43**, 101105 (2021)
12. Shi, S., Fei, Z., Karimi, H.R., Lam, H.-K.: Event-triggered control for switched T-S fuzzy systems with general asynchronism. IEEE Trans. Fuzzy Syst. **30**(1), 27–38 (2022)
13. Wang, T., Tong, S.: Observer-based output-feedback asynchronous control for switched fuzzy systems. IEEE Trans. Cybern. **47**(9), 2579–2591 (2017)
14. Li, S., Xiang, Z.: Exponential stability analysis and L_2-gain control synthesis for positive switched T-S fuzzy systems. Nonlinear Anal. Hybrid Syst. **27**, 77–91 (2018)
15. Zhang, M., Shi, P., Shen, C., Wu, Z.G.: Static output feedback control of switched nonlinear systems with actuator faults. IEEE Trans. Fuzzy Syst. **28**(8), 1600–1609 (2020)
16. Shi, S., Fei, Z., Shi, P., Ahn, C.K.: Asynchronous filtering for discrete-time switched T-S fuzzy systems. IEEE Trans. Fuzzy Syst. **28**(8), 1531–1541 (2020)
17. Fei, Z., Shi, S., Wang, T., Ahn, C.K.: Improved stability criteria for discrete-time switched T-S fuzzy systems. IEEE Trans. Syst. Man Cybern. **51**(2), 712–720 (2021)
18. Bao, Z., Lam, H., Peng, Y., Liu, F., Mehran, K.: Stability and stabilization of polynomial fuzzy-model-based switched nonlinear systems under MDADT switching signal. IEEE Trans. Fuzzy Syst. **31**(1), 1–13 (2023)
19. Li, X., Shan, Y., Lam, H.-K., Bao, Z., Zhao, J.: Exponential stabilization of polynomial fuzzy positive switched systems with time delay considering MDADT switching signal. IEEE Trans. Fuzzy Syst. **32**(1), 174–187 (2024)
20. Sala, A., Ariño, C.: Asymptotically necessary and sufficient conditions for stability and performance in fuzzy control: applications of Polya's theorem. Fuzzy Sets Syst. **158**(24), 2671–2686 (2007)
21. Chen, Y.-J., Tanaka, K., Tanaka, M., Tsai, S.-H., Wang, H.O.: A novel path-following-method-based polynomial fuzzy control design. IEEE Trans. Cybern. **51**(6), 2993–3003 (2021)
22. Bao, Z., Li, X., Lam, H.K., Peng, Y., Liu, F.: Membership-function-dependent stability analysis for polynomial-fuzzy-model-based control systems via Chebyshev membership functions. IEEE Trans. Fuzzy Syst. **29**(11), 3280–3292 (2021)
23. Zhang, L., Gao, H.: Asynchronously switched control of switched linear systems with average dwell time. Automatica **46**(5), 953–958 (2010)
24. Liu, C., Li, Y., Zheng, Q., Zhang, H.: Non-weighted L_2 gain and asynchronous H_∞ control for continuous-time switched T-S fuzzy systems. ISA Trans. **103**, 228–236 (2020)
25. Lam, H.K., Lauber, J.: Membership-function-dependent stability analysis of fuzzy-model-based control systems using fuzzy Lyapunov functions. Inf. Sci. **232**, 253–266 (2013)
26. Yang, J., Zhao, X., Bu, X., Qian, W.: Stabilization of switched linear systems via admissible edge-dependent switching signals. Nonlinear Anal. Hybrid Syst. **29**, 100–109 (2018)
27. Lam, H.K.: A review on stability analysis of continuous-time fuzzy-model-based control systems: from membership-function-independent to membership-function-dependent analysis. Eng. Appl. Artif. Intell. **67**, 390–408 (2018)
28. Yuan, S., Zhang, L., De Schutter, B., Baldi, S.: A novel Lyapunov function for a non-weighted L_2 gain of asynchronously switched linear systems. Automatica **87**, 310–317 (2018)
29. Lo, J.-C., Lin, C.: Polynomial fuzzy observed-state feedback stabilization via homogeneous Lyapunov methods. IEEE Trans. Fuzzy Syst. **26**(5), 2873–2885 (2018)
30. Jiang, B., Karimi, H.R., Kao, Y., Gao, C.: Takagi-Sugeno model based event-triggered fuzzy sliding-mode control of networked control systems with semi-markovian switchings. IEEE Trans. Fuzzy Syst. **28**(4), 673–683 (2020)

Zhiyong Bao received the B.S. and the Ph.D. degrees in Instrument Science and Technology from Yanshan University, Qinhuangdao, China, in 2013 and 2022, respectively. He is currently a lecturer with the School of Electrical Engineering, Yanshan University, China. His research interests include switched systems, polynomial fuzzy model-based system, and intelligent control.

Hak Keung Lam (Fellow, IEEE) received the B.Eng. (Hons.) and Ph.D. degrees from the Department of Electronic and Information Engineering, Hong Kong Polytechnic University, Hong Kong, in 1995 and 2000, respectively. From 2000 and 2005, he was with the Department of Electronic and Information Engineering, Hong Kong Polytechnic University, Hong Kong, as a Postdoctoral Fellow and a Research Fellow, respectively. In 2005, he joined as a Lecturer with Kings College London, London, U.K., where he is currently a Reader. He has coedited two edited volumes: Control of Chaotic Nonlinear Circuits (World Scientific, 2009) and Computational Intelligence and Its Applications (World Scientific, 2012), and authored/coauthored three monographs: Stability Analysis of Fuzzy Model-Based Control Systems (Springer, 2011), Polynomial Fuzzy Model-Based Control Systems (Springer, 2016), and Analysis and Synthesis for Interval Type 2 Fuzzy Model-Based Systems (Springer, 2016). His current research interests include intelligent control and computational intelligence. Dr. Lam is currently the Program Committee Member, the International Advisory Board Member, the Invited Session Chair, and the Publication Chair for various international conferences, and a Reviewer for various books, international journals, and international conferences. He was an Associate Editor for IEEE Transactions on Circuits and Systems Part II: Express Briefs and IEEE Transactions on Fuzzy Systems. He is currently an Associate Editor for IET Control Theory and Applications, International Journal of Fuzzy Systems, Neurocomputing, and Nonlinear Dynamics, and a Guest Editor/Editorial Board for a number of international journals. He was named as a highly cited Researcher by the Web of Science.

Xiaomiao Li received the B.Eng. degree in Automation from Yanshan University, Qinhuangdao, China, in 2014 , and Ph.D. degrees from the School of Electronic Engineering and Computer Science, Queen Mary University of London, UK, in 2021. She is currently a vice Professor with the Department of Automation, School of Electrical Engineering, Yanshan University, China. Her research interests include stability analysis for fuzzy positive systems, polynomial fuzzy model-based system, and intelligent control.

Fucai Liu received the B.S. and M.S. degrees from the Department of Automation, Northeast Heavy Mechanism Academe, Qiqihar, China, in 1989 and 1994, and the Ph.D. degree from the Department of Control Science and Engineering, Harbin Institute of Technology, Harbin, China, in 2003. He is currently a Professor with the Department of Automation, School of Electrical Engineering, Yanshan University, Qinhuangdao, China. He is also the Director of Hebei Automation Experimental Teaching Demonstration Center. He has authored/coauth ored more than 280 papers in mathematical, technical journals, and conferences. He is the author of the book Fuzzy Model Identification for Nonlinear Systems and Its Applications. His research interests include spatial mechanism behavior analysis and control, stability analysis for fuzzy positive systems, fuzzy identification, and control of nonlinear systems, etc.